MegaWave™ CORPORATION

UNCLASSIFIED

Final Technical Report
"Innovative Soldier Conformal Antenna Suite"

29 June 2001

Contract No. DAAD16-01-C-0007

Prepared for:

United States Army
Individual Protection Teams
Multi-Functional Material Team
Kansas Street
Natick, MA 01760

Prepared by:

MegaWave Corporation
200 Shrewsbury Street
P.O. Box 614
Boylston, MA 01505

Principal Investigator: Marshall W. Cross

UNCLASSIFIED

REPORT DOCUMENTATION PAGE	*Form Approved OMB No. 0704-0188*

1. AGENCY USE ONLY (Leave blank)	2. REPORT DATE	3. REPORT TYPE AND DATES COVERED
	June 29, 2001	Final Scientific and Technical

4. TITLE AND SUBTITLE	5. FUNDING NUMBERS
Innovative Soldier Conformal VHF/UHF Antenna Suite	Contract # DAAD16-01-C-0007
6. AUTHOR(S)	
Cross, Marshall W., Benham, Glynda O. and Row, Dr. Ronald V.	

7. PERFORMING ORGANIZATION NAME(S) AND ADDRESS(ES)	8. PERFORMING ORGANIZATION REPORT NUMBER
MegaWave Corporation 200 Shrewsbury Street, P.O. Box 614 Boylston, MA 01505	NAT01-001

9. SPONSORING/MONITORING AGENCY NAME(S) AND ADDRESS(ES)	10. SPONSORING/MONITORING AGENCY REPORT NUMBER
United States Army W13G07, Individual Protection Teams Multifunctional Material Team Kansas Street Natick, MA 01760 Mr. James Fairneny 5209	CLIN 0001AB Data Item A002

11. SUPPLEMENTARY NOTES
SBIR Phase I Report Topic Number A00-072

12a. DISTRIBUTION/AVAILABILITY STATEMENT	12b. DISTRIBUTION CODE
Approved for Public Release, Distribution Unlimited	

13. ABSTRACT (Maximum 200 words)

The electrical characteristics and radiation performance of: multiple, Tesla-series connected, bifilar-wound coils around flexible magnetic cores worn around the back half of the waist at VHF and UHF monopoles over artificial dielectric ground planes were computed and verified by laboratory measurements. It was found that at low VHF the Tesla configured loops exhibited significant bandwidth and efficiency advantages over conventional ones and worthwhile gains at UHF were both predicted and measured when one-wavelength diameter artificial dielectric ground planes were used under the shoulder-mounted monopoles.

14. SUBJECT TERMS	15. NUMBER OF PAGES
VHF/UHF conformal antennas, artificial dielectrics, series bifilar wound helices, wearable antennas, self-organizing antenna systems, bed-of-pins ground planes	40
	16. PRICE CODE

17. SECURITY CLASSIFICATION OF REPORT	18. SECURITY CLASSIFICATION OF THIS PAGE	19. SECURITY CLASSIFICATION OF ABSTRACT	20. LIMITATION OF ABSTRACT
Unclas	Unclas	Unclas	SAR

NSN 7540-01-280-5500

Standard Form 298 (Rev. 2-89)
Prescribed by ANSI Std. 239-18

Table of Contents

List of Figures and Tables

1.0 Summary

Existing antennas connected to soldier-carried VHF/UHF radio transceivers are not conformal to the soldier's body, visually covert or robust and their radiation patterns and dominant polarization are largely determined by the soldier's position. This limits, rather than enhances, a warfighter's mobility and ability to communicate. The development and fielding of compact, belt-worn radios also requires a shift from conventional to better performing body conformal antennas.

Working with the government Program Manager we developed a set of desired characteristics and performance goals for a VHF (30-88 MHz) and UHF (1755-2500 MHz) soldier conformal antenna suite then established the technical feasibility of several innovative designs based on: a literature search, computer modeling and some initial laboratory experiments. In the VHF band we found that series-bifilar wound Tesla coils, when operated above their first self-resonant frequency (SRF): exhibited orders of magnitude increase in bandwidth without a decrease in efficiency; demonstrated their ability to effectively operate with magnetic cores intended to guide the flux into the body at waist level turning the soldier into an efficient VHF antenna; and when arranged as a set of critically coupled windings on a common core, provided nearly 1.5 octaves of bandwidth without the need for active tuning. For the UHF band we have found that a thin pin bed or dielectric ground plane structure a few inches in radius will greatly enhance an antenna's surfacewave fields, allow a tailoring of the radiation patterns and reduce the specific absorption rate (SAR) in a soldier's body. Using emerging MEMS electromechanical RF switching technology, several UHF elements over flexible pin beds or dielectric ground planes located on or near the shoulders, results in the desired mixed-polarization pattern, independent of the position or orientation of a soldier.

We have concluded that our Phase I theoretical and preliminary experimental work strongly indicates the technical and operational feasibility of fabricating a soldier conformal, soldier position/orientation independent antenna suite covering the 30-88 and 1755-2500 MHz radio bands, capable of being integrated into worn equipment such as the MOLLE. This suite will include a high performance, conformal waist mounted loop antenna for VHF and UHF shoulder worn elements that will adapt to the warfighter's body position and whose performance is significantly enhanced by the use of artificial ground planes. A conceptual implementation of the soldier conformal antenna suite is shown in Figure 1-1. Operation in both bands will not require any modifications to, or redesign of, existing or planned transceivers.

Based upon our work over the past six months, we recommend that the soldier conformal antenna suite be transitioned from the mostly theoretical and limited experimental phase reported on herein to a final, tested and fully characterized prototype conformal antenna suite suitable for link testing and demonstration to government and private sector users.

2.0 Introduction

A conformal, or as sometimes termed "low-profile" antenna is one that is shaped so that considerable size reduction is realized in one plane. It may or may not be an electrically small antenna: one that can be physically bounded by a sphere having a radius equal to approximately 5/32nds of a wavelength. In the 30-88 MHz band the wavelength varies between 10 and 3.4 meters and between 0.17 and 0.12 meters across the 1755 to 2500 MHz range. Any practical body-conformal antenna for the VHF band will be electrically small, while antennas for the UHF range of interest will be physically rather than electrically small but still conformal in that they must not protrude materially from the surface of a host carrier such as the MOLLE.

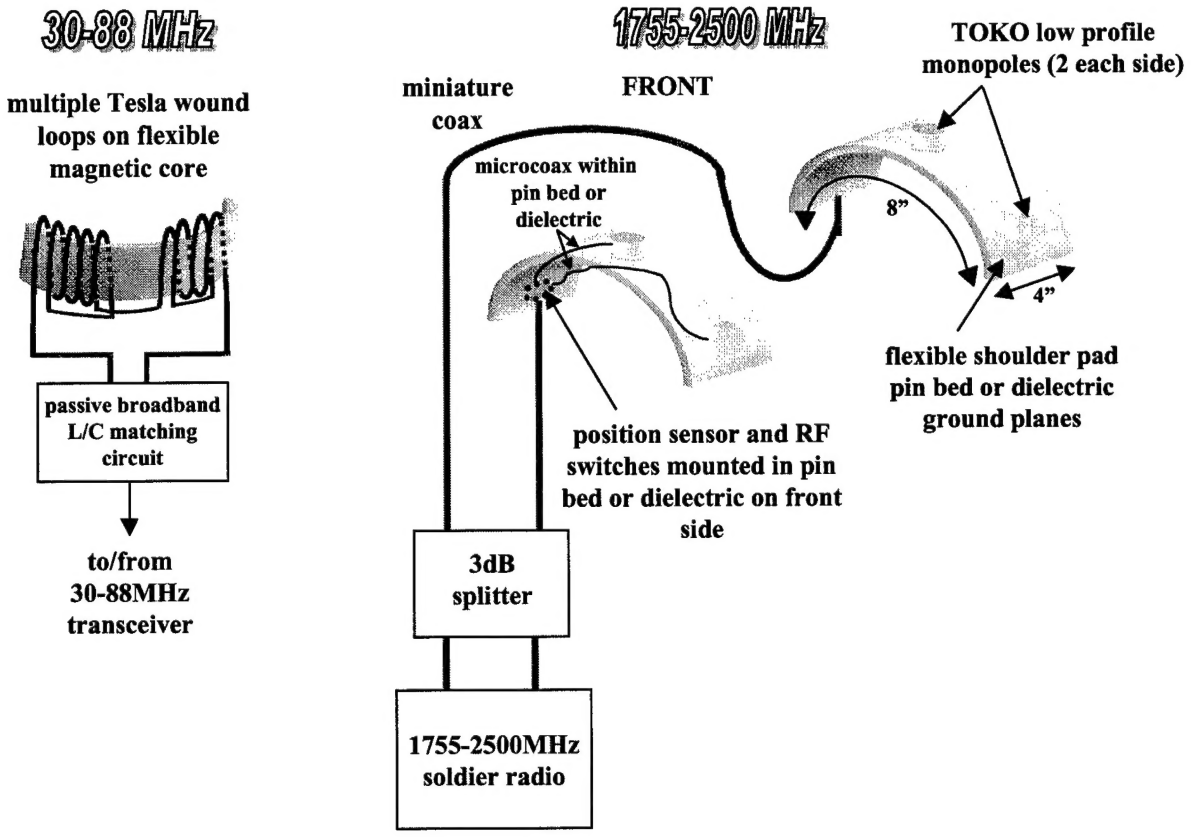

Figure 1-1 Possible Advanced Prototype Soldier Conformal Antenna Suite Configuration

It has been well established through theory and measurement that many types of antennas located in close proximity to the human body are inefficient, especially at VHF due to high dielectric losses. Previous work, identified in Section 4, has established that the body itself can be used as an effective, essentially omnidirectional antenna in the VHF band of interest by connecting the radio transceiver to a tuned, narrow-band loop placed orthogonally against the torso. Using this configuration the resulting radiated fields are many times stronger than from the loop alone, proving that the body, which is electrically resonant in the 30-88 MHz band, is the prime radiator and not the loop. The challenge in devising a practical system based on this technique lies in the development of a conformal loop with high (58 MHz or 1.5 octave) bandwidth capable of efficiently coupling magnetic flux into the human body. A little known US Patent (#512,340) entitled "Coil for Electromagnets" granted to Nikola Tesla in 1894 and first pointed-out to this project's principal investigator by Mr. Oliver Nichelson of the Eyring Research Institute in 1990, describes a bifilar winding in which the end of the first winding is connected in series to the beginning of the second winding. Tesla goes on to show that this winding scheme yields a more efficient coil than a conventionally wound one and was a stage in the inventor's attempts to reduce long distance power transmission losses through the use of resonant circuits. At radio frequencies, it appears to offer exactly what is required for a body-coupled loop operating at low VHF. By placing the Tesla configured windings around a small diameter, flexible magnetic core, the resulting flux, which is concentrated within the core, is forced to flow through the body by bending its ends toward the waist. When standing or kneeling this scheme will produce an essentially omniazimuthal vertically polarized radiation pattern. When the soldier is in the prone position, a mixed vertical/horizontally polarized radiation pattern will be developed due to the refractive properties of the earth at VHF as noted by many researchers during the past century, beginning with Rogers' seminal work (US Patent #1,303,730) in 1919.

Unlike operation in the 30-88 MHz band, the human body and its appendages tend to shield or "block" radiation in the 1755-2500 MHz portion of the UHF band. Thus the key challenge is not only to design conformal antennas that must work efficiently in close proximity to the body but also to provide adequate radiation pattern coverage for all azimuthal orientations and positions (standing-to-prone) while simultaneously minimizing UHF radiation (expressed as the SAR) into the body and organs of a soldier. One technique to increase an antenna's efficiency when located near a lossy surface that has received very limited past consideration is the use of artificial dielectric ground planes of finite size under short, vertically polarized monopoles, as noticed by this project's principal investigator at the 1988 I.E.E. High Frequency (HF) Symposium in London. The authors of a paper given at this conference showed by experiment that the HF surfacewave component could be enhanced by an array of short vertical conductors under an antenna element, as was predicted and observed at microwave frequencies in two earlier (1980's) papers by Ray King and his colleagues. They described the use of a fakir's bed of pins to produce an inductive surface impedance (as codified in Kay's and Wait's work in the 1960s) which in turn resulted in an enhanced surfacewave component. By integrating the bed of pins and a dielectrically loaded short monopole into thin, flexible foam shoulder pads and using gravity operated position sensors controlling MEMS electromechanical RF switches to select the optimum antenna element for a given soldier's position, an essentially omniazimuthal, position independent conformal antenna system that radiates mixed polarizations and is decoupled from the human body will be realized.

Artificial ground planes can also be rendered in several other ways as illustrated in Figure 2-1 using a dielectric layer over a perfectly conducting ground; via corrugations; using a "pin-bed" or fakir's bed of nails as described above; and frequency selective surfaces (FSS). Efforts by other researchers using FSS techniques in the same band have yielded structures that are several inches thick and 12"x16" inches in lateral extent which cannot be practically accommodated on the soldier's body. Corrugations have similar properties to the other periodic structures. The two techniques focused on were the dielectric layer and the pin bed since they would have thicknesses appropriate for a conformal antenna elements.

The overall objective of our Phase I research was to establish the technical feasibility of the above techniques leading to the soldier conformal antenna suite capable of efficient operation in the 30-88 MHz (VHF) and 1755-2500 MHz (UHF) bands and being integrated into worn equipment such as the MOLLE. The methods and procedures used to accomplish this are described in the following section (3.0). The majority of this report is then devoted to a discussion of the results of our Phase I research which is found in Section 4, followed by conclusions and recommendations in Sections 5 and 6 respectively.

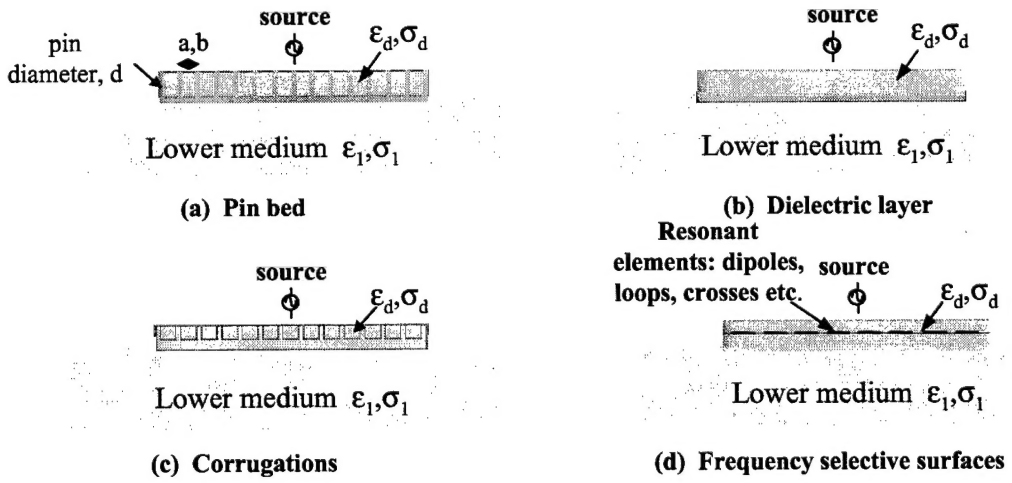

Figure 2-1 Types of artificial ground planes

3.0 Methods, Assumptions and Procedures

This section discusses the methods and procedures used to evaluate the feasibility of the following innovative techniques:

- Small, flexible magnetic cores around which multiple, coupled helical metal ribbons are wound as Tesla-series bifilar coils, each designed to magnetically couple with the body providing position and orientation independent, omni-directional, mixed polarization coverage across the 30-88MHz band. As envisioned, this antenna would be incorporated into the back half of the MOLLE's waist belt and be designed to link the maximum magnetic flux into the body to take advantage of the latter's ability to act as an efficient antenna within this band.
- Dielectrically-loaded short monopoles or grounded-line elements fed against low-profile, flexible, artificial dielectric ("reactive") ground planes which have the potential to increase radiation efficiency of UHF antennas near a human body while reducing SAR and providing some amount of space diversity gain. It is also proposed that performance will be improved due to the more efficient launching of a surfacewave along the body by the reactive ground plane.
- Miniature electromechanical or electronic switches controlled by gravity operated position sensors to select the optimum shoulder mounted UHF antenna or combination of antennas to achieve the desired omnidirectional coverage regardless of the warfighter's position (standing to prone) or orientation.

The key assumption made in order to evaluate the above was that real estate on the MOLLE fighting load vest or other existing or planned worn equipment items would be available so that the resulting VHF and UHF conformal antenna elements, position sensors, switches and cables could be integrated at locations that would minimize the effect of the soldier's body and other worn equipment to the radiation patterns of the antennas. It was also assumed that the performance goals and desired physical and electrical characteristics listed in Section 4.1 of this report and supplied as an interim report in February, 2001 were acceptable.

The key technical issues that were addressed to determine technical feasibility of the above techniques were:

- 30-88 MHz: Radiation efficiency/pattern/polarization vs. soldier position/orientation, instantaneous bandwidth and wearability (size/shape/volume/weight)
- 1755-2500 MHz: The gain realized using an artificial dielectric ground plane whose diameter is on the order of one-wavelength versus a conventional metallic one of the same diameter and the degree to which an enhanced surfacewave is launched along the body while in the prone position.
- The availability, electrical performance and physical robustness of miniature gravity actuated position sensors/switches required to control the multiple 1755-2500 MHz elements located on/near a warfighter's shoulders.

In order to accomplish the above we attended a kickoff meeting with the government Program Manager to review performance goals for the antenna suite; initiated a literature search in the three general areas listed above; conducted extensive computer modeling, analytical treatment and initial experiments with artificial dielectric ground plane antennas; performed an analysis followed by limited laboratory measurements of various 30-88 MHz body-coupled, helically wound configurations; and held meetings with several manufacturers of miniature electrical-mechanical and solid-state RF switches. The results of the January, 2001 meeting with the Project Manager were documented in [1], and included here as Section 4.1 which contains the desired operational, physical and environmental characteristics as well as electrical performance goals for the conformal antenna suite.

The literature search was conducted at the US Air Force Research Library, Hanscom AFB and the Worcester Polytechnic Institute's Gordon Library and yielded over two-dozen directly relevant papers dealing with: artificial dielectric/inhomogeneous ground planes, the effects of the human body on VHF antenna patterns and efficiency, VHF RF applicators for hyperthermia treatment, the frequency response of multiple-coupled coils, magnetically loaded helical VHF antennas and the performance of solid-state RF switches. No information (beyond his 1894 patent [2]) was discovered regarding the Tesla series-bifilar-wound RF coil.

The majority of our work was concerned with the analysis and modeling of pinned and dielectric ground planes. The pin bed was firstly analyzed using the NEC-4 Moment Method Code [3]. The dielectric layer was modeled using the Finite Difference Time Domain Code XFDTD [4] since dielectric layers of finite extent cannot be handled by the NEC code. In addition, MathCAD [5] documents were implemented based on Wait's compensation method formulation [6] for both the pin bed and dielectric layer structures. These three methods are illustrated in Figures 3-1(a)-(c). Figure 3-1(a) shows the NEC pin bed model used. A square gridded ground plane 4" square was modeled and the pins modeled as wires attached to the ground plane at the grid intersection points. The ground plane was located at the air-dielectric interface at z=0. The Sommerfeld option was used in the computation since wires lie on the interface. A dielectric constant of 4 and conductivity of 0 was applied to the lower medium. The vertical electric fields were computed using the NE and the RP1 options in NEC. NE computes the near fields and RP1 computes the total fields including the surfacewave. The fields were compared with the pins and without the pins included in the model.

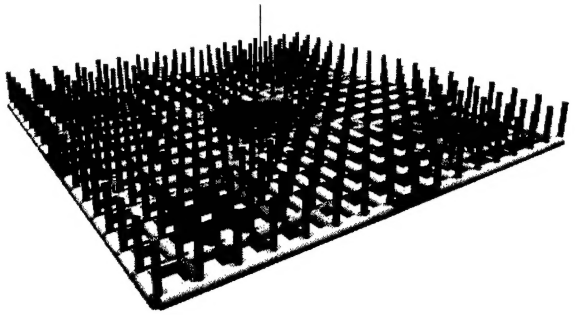

Figure 3-1(a) NEC-4 Pin Bed Model

In the XFDTD model shown in Figure 3-1(b), the lower half of the XFDTD solution space was filled with a dielectric, a 4" diameter metallic ground screen was placed at the air-earth interface and the dielectric layer placed directly on top of the ground screen. A short dipole was used as the source in this case with the lower end of the source placed one cell away from the upper surface of the dielectric. A sinusoidal waveform was used as the source excitation to obtain results at a single frequency. The fields near the edge of the metallic ground screen were computed and compared with and without the dielectric layer.

In Wait's method, illustrated in general terms in Figure 3-1(c) conducting, pinned or dielectric covered ground screens are introduced via an equivalent normalized surface impedance and compared to the "no ground screen case". In Wait's analysis, the source was again assumed to be an electrically short current element at zero height. Wait's method involves the evaluation of a gain factor due to a general ground screen, Ωa given by:

$$\Omega a := \left[\int_0^{2\cdot\pi\cdot\frac{s}{\lambda}} F(u)\,du + \left(\frac{1}{i}\right)\cdot \int_0^{2\cdot\pi\cdot\frac{s}{\lambda}} \left(\frac{1}{u}\right)\cdot F(u)\,du \right] \cdot \frac{(Zn - Znorm)}{\cos(\Psi)} \qquad \ldots\ldots (1)$$

where s = ground screen radius
λ = wavelength
ψ = angle of elevation to the observer
Z_{norm} = normalized surface impedance of the lower medium
Z_n = normalized surface impedance of the ground screen

If the ground screen in a perfectly conducting screen, then $Z_n=0$. The form of Z_n for both the pin bed and dielectric layer structures is as follows. The surface impedance for the pinned case was determined using King et al's approach [7] which ultimately shows the normalized reactance of the pin bed X_{np} to be given by:

$$X_{np} = k_{z1} \tan (k_{z1}.t)/ \varepsilon_x.k_x$$

where k_{z1} = vertical wavenumber
t = height of the pin bed
ε_x = equivalent dielectric constant in x-direction with pins in place
k_x = lateral wavenumber

For the dielectric layer case, the normalized surface reactance X_{nd} is shown by Wait to be given by:

$$X_{nd} = \tan [k\, t \sqrt{\{\eta_d - \cos^2\psi\}}].\sqrt{\{\eta_d - \cos^2\psi\}}/\eta_d$$

where k = wavenumber in the dielectric
t = thickness of the dielectric
η_d = square of the refractive index of the dielectric
ψ = elevation angle to observer

It is therefore seen that the normalized surface reactances of both the pin bed and the dielectric layer take the same form, both involving the tangent of some function multiplied by the thickness of the pin bed or dielectric layer. The Wait MathCAD analysis was also developed to allow for the pin bed to be embedded in a dielectric material defined by its dielectric constant ε_d.

MathCAD was used to evaluate Wait's integrals and the equivalent surface impedance for a pin bed case, a ground screen covered with a dielectric layer and also the elevation patterns for the dielectric layer case. The MathCAD documents are provided as part of this report in Appendices A, B and C.

In certain instances limited laboratory measurements were made in order to:

- Resolve differences between and confirm results of analysis and modeling
- Determine electrical characteristics where analysis and modeling are not practical.

Two calibrated instruments were used to accomplish the above measurements: HP-8753C Vector Network Analyzer (VNA) and its 85024A High Impedance Probe and the HP-8591E Spectrum Analyzer. They were used to characterize (complex impedance, VSWR and insertion loss) and measure both flux as well as gain/efficiency of the various loop designs and relative gain for the pin bed ground planes. The following section includes the details of the measurements made, using the above equipment, to confirm our analytical work.

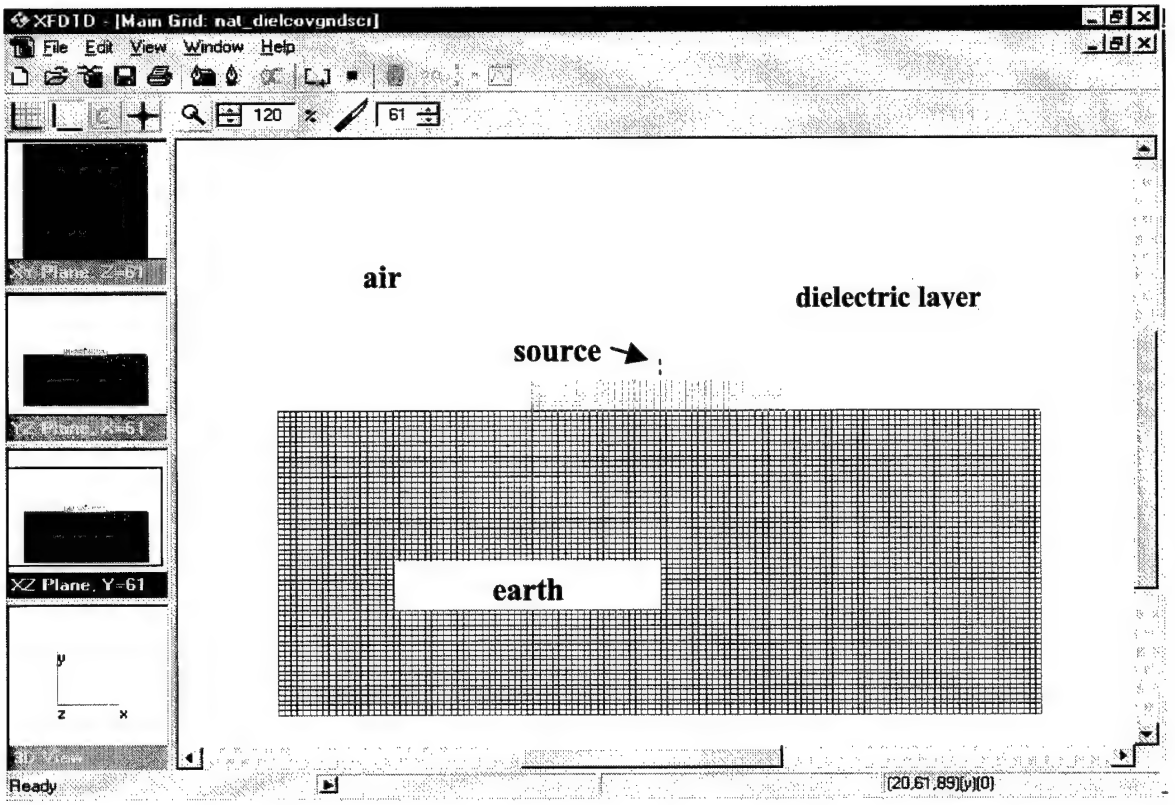

Figure 3-1(b) XFDTD model of dielectric layer covered ground screen

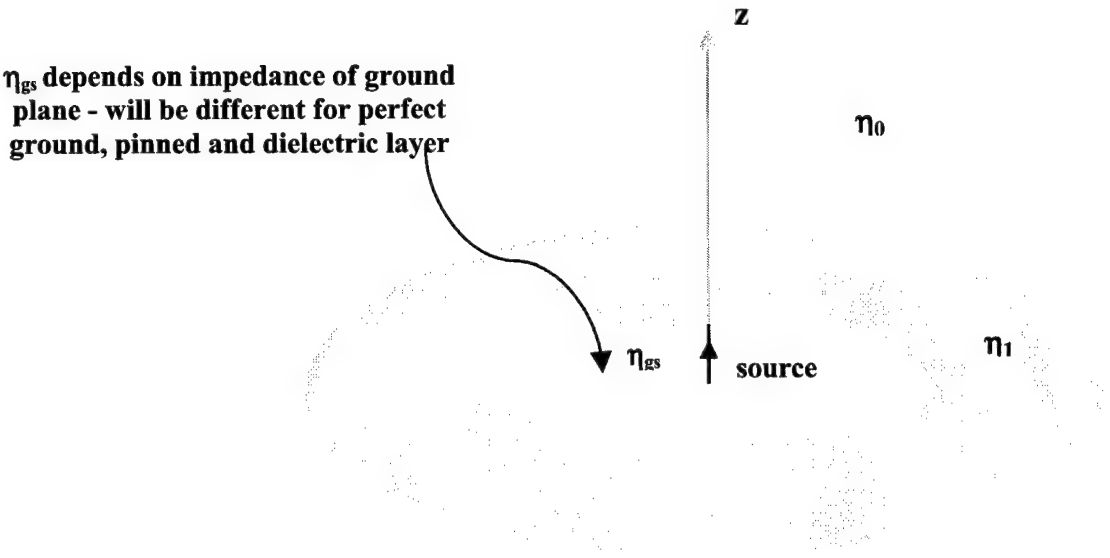

Figure 3-1(c) Illustration of Wait's Method

4.0 Results and Discussion

4.1 Performance Goals and Characteristics

The objective of Task 1 of this Phase I contract was to establish categories and target performance values for operational/environmental goals and physical/electrical characteristics for military use of the soldier conformal VHF/UHF antenna suite. They were developed based upon: the original A00-072 project solicitation; discussions with the Program Manager, Mr. James Fairneny on 10 January, 2001 and a review of MegaWave's work on: the DARPA-LISA; SSC MOUT ACTD-ACE and SSC Soldier Worn Antenna BAA Contract. The categories of military performance goals that we have identified are listed below and target performance values are provided for each category.

Military Operational/Environmental

- Host system: MOLLE fighting load vest
- Soldier positions: standing, kneeling and prone on ground and structures
- MOLLE mounting locations: VHF (SINCGARS) on MOLLE vest at waist level near the quick release frame fixture; UHF (soldier radio/ISM) on/near MOLLE vest shoulder straps.
- Soldier safety: EM-SAR (ANSI/IEEE C95.3-1992) for controlled exposure.
- Temperature: operating -30 to +50 degrees C, storage -50 to +50 degrees C.
- Humidity: 0-100% to include rain and occasional immersion.

The antenna suite must be capable of withstanding the shock, vibration and flexure encountered during all realistic conditions of: storage, transportation, use while on a soldier in transit, garrison and battle and during field maintenance and cleaning. The antenna suite must also be protected from abrasion cause by MOLLE-carried loads, be compatible with body armor and CBW gear and be free from any sharp protuberances.

Physical and Electrical

- Frequency bands: 30-88 MHz (SINCGARS), 1755-1850 MHz (soldier radio) and 2400-2500 MHz (ISM).
- Simultaneous Operation (SIMOP): any and all combinations of the above bands.
- Feeds: one for each band.
- Instantaneous bandwidths: across the bands listed above without the need for electrical or mechanical tuning.
- Polarization: dual (approximately equal excitation of TM and TE) regardless of soldier position (standing to prone) and orientation.
- Impedance: 50 ohms (nominal).
- VSWR: 2.5:1 or less over each frequency band listed above.
- Azimuthal pattern: omnidirectional with less than +/- 6dB of pattern ripple regardless of soldier position (standing to prone) or orientation.
- Power gain: 30 MHz >-6dBi, 45 MHz >-3dBi, 88MHz >0dBi; 1755-2500 MHz >0dBi.
- Prime power consumption: zero
- Power handling capability: 10 watts 30-88 MHz, 0.75 watts 1755-2500 MHz.
- Weight: total suite (antennas/cables/connectors) <150 grams.
- Size: capable of being integrated into the MOLLE system with maximum protuberance of less than 20mm.

4.2 30-88 MHz, Body-Coupled, Multiple, Tesla Series Wound, Magnetically-Loaded Helical Loop Antennas

The ideal antenna for this band would have a reasonable power gain (-6 dBi at 30 MHz, increasing to 0 dBi at 88 MHz) and an instantaneous bandwidth of 58 MHz (1.5 octaves) without any type of active mechanical or electrical tuning. It would also be capable of taking advantage of the well-known body enhancement exhibited by magnetic (loop) antennas mounted orthogonally to the torso, have a dual-polarized, omni-azimuthal radiation pattern regardless of the soldier's position (standing-to-prone)/orientation and be low in profile (conformal), weight and volume.

The literature has established the following generally accepted principles, which either aid in or hinder achieving the desired characteristics and performance:

- The human body is electrically resonant in the 30-88 MHz band of interest [8].

- A loop ("H"-field) antenna, whose axis is tangential to the mostly conductive human body produces the most effective excitation of in-body currents which results in the body acting more as an antenna than an absorber. This fact is reported in [8, 9, 10, 11 and 12] which deal with antennas and [13, 14] which discuss the use of loops as RF "applicators" located adjacent to or wound around the human body for hyperthermia treatment of tumors.

- Electrically small multi-turn loops, conventionally-wound and volumetrically constrained (helices), suffer from losses (effective loss resistances orders of magnitude greater than their radiation resistances). These are due to: the proximity effect which can, at low VHF, exceed skin effect losses by a factor of 2-3 depending upon the coil's geometry and relative dimensions [15], and if magnetically loaded, from magnetic and dielectric losses typical of ferrite or iron powder cores [16].

- However the above class of loops exhibits increased radiation efficiencies (ratio of radiated power to total input power to the loop) up to 10 dB in our band of interest when they are magnetically loaded [16]. The magnetic cores also constrain the flux to flow along them, which suggests the possibility of "guiding" the flux into the body [17]. Their radiation efficiencies and bandwidths can also be significantly increased using multi-turn structures [18] and the Tesla series connected, bifilar-wound configuration [19].

The design of a practical low-profile (conformal) body-worn 30-88 MHz antenna requires a detailed study of the above by trading one effect for another to obtain the highest value of gain for a given volume while at the same time providing a feed-point impedance that is capable of being efficiently matched over the desired band using passive components. We divided our Phase I VHF band efforts into four sequential subtasks:

- Verifying the theoretical gains, patterns and bandwidths of conventionally wound, multi-turn, air-core loops near the human body when their planes are orthogonal to the body. (Section 4.2.1)
- Evaluating the effect of magnetic cores on these loops: gain and bandwidth as well as the amount of "flux-guiding". (Section 4.2.2)
- Investigating the effect of implementing the above using Tesla series connected bifilar windings on gain and bandwidth. (Section 4.2.3)
- Determining the feasibility of using separate, multiple, critically-coupled Tesla-wound coils on a common core to improve bandwidth while not materially affecting gain. (Section 4.2.4)

4.2.1 Conventionally-Wound, Air-Core Loops

Using the experimental setup and loop configuration shown in Figure 4.2-1, the 3dB bandwidth of the loop was measured to be 483 kHz when the loop was tuned to resonance at 59 MHz and matched to 1:1 VSWR (50 ohms) by connecting the coax's center conductor 4.8 cm from the coil's center (also connected to the coax's shield). Using the equations due to Smith [15], the computed bandwidth was determined to be 426 kHz. When the loop was placed so it was orthogonal to and 5 mm from the waist of a human, its computed and measured bandwidths increased to 705 and 988 kHz respectively. The computed and measured gain enhancements of the body were +11.1 and +13.8 dB respectively, with less than +/-1.2 dB of ripple when the body was rotated through 360 degrees, values consistent with those reported in the above literature. This indicates that the excellent coupling to and resulting use of the body as a "virtual" antenna greatly exceeds the increased losses that are indicated by the increased bandwidths (lowered Q) due to losses in the body.

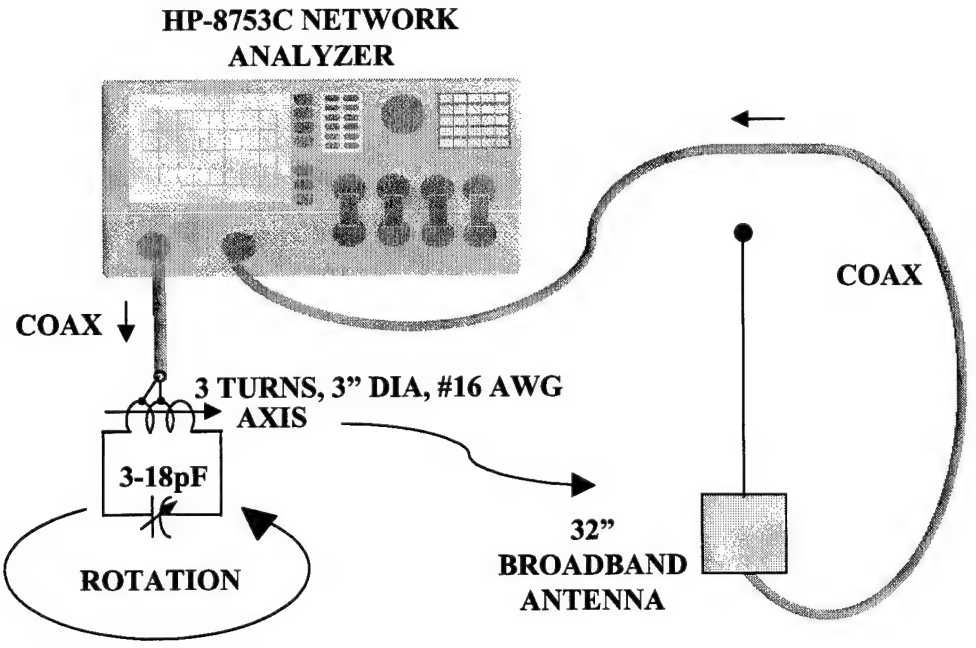

Figure 4.2-1 Conventional Loop Experimental Setup

4.2.2 Effect of Magnetic Cores on Conventionally-Wound Loops

Various ferrite and iron powder cores, some of which are shown in Figure 4.2-2 were evaluated using the above loop by threading the core through the loop's plane. These included: Amidon materials # 2 and 10; Cuming Corp. C-RAM FLX-1.0; Fair-Rite materials #67 and 68, and Capcon LST-225. Using the equations due to DeVore and Bohley [Appendices A and B, ref. 16] the change in the 3 dB bandwidths were computed and confirmed by measurement using their procedure and the HP-8753C Vector Network Analyzer (VNA). The change in bandwidth and gain are listed in Table 4.2-1.

Material	Change in Bandwidth (%)		Change in Gain (dB)	
# type	Calculated	Measured	Calculated	Measured
#10 (Amidon)	+107	+166	+0.6	-1.8
FLX-1.0 (Cuming)	+43	+78	+1.9	+0.7
#2 (Amidon)	+85	+56	+3.4	+2.7
67 (Fair-Rite)	+390	+530	-2.6	-5.5
68 (Fair-Rite)	+205	+282	-1.4	-3.2
LST225 (Capcon)	+180	+164	-1.1	-4.3

Table 4.2-1: Evaluation of the Effects of Magnetic Loading

From the above initial analysis and measurements, conducted at mid-band (59 MHz), it is apparent that the losses of all magnetic materials except Amidon iron powder #2 and Cuming FLX-1.0 exceed any increase in radiation resistance for the loop. Even for these materials the gain is much less than reported in the literature for the 3-30 MHz band, indicating the effect of the steep rise in the manufacturers' published loss factor curves in the VHF band. This finding confirms the need to continue to search for efficient magnetic materials in the low VHF band during any Phase II effort.

In order to evaluate the degree of "flux-guiding" that a magnetic core provides two experiments were performed. The first involved the construction of a magnetic flux sensor using the HP-85024A High Impedance Probe by adding a 10 mm diameter, 3 turn loop to its tip which replaced the 32" broadband E-field sensor antenna shown in Figure 4.2-1 connected to port 2 on the 8753C VNA. A conventionally wound coil consisting of 20 turns of #16 insulated wire on the Amidon #2 iron powder semi-circular core (25 x 20 mm cross section) was connected to port 1 of the VNA and the flux sensor was used to map its relative strength (the sensor and coil are shown in Figure 4.2-3). The resulting relative strength, as a function of radial distance from the core's center is plotted in Figure 4.2-4 which indicates that the curved core will guide the flux into the body.

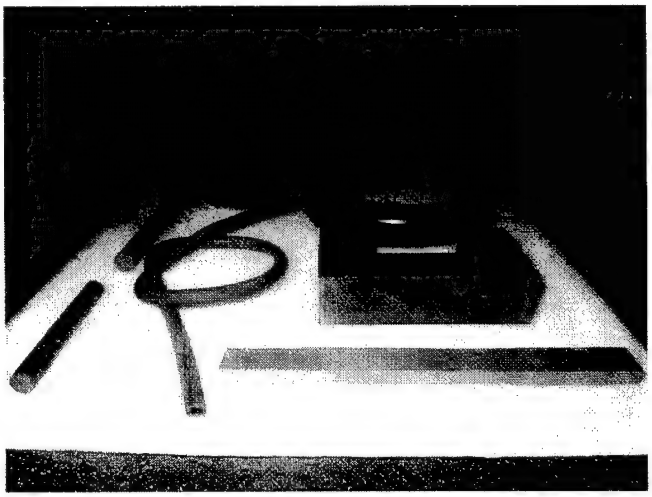

Figure 4.2-2 Ferrite and Iron Powder Core Samples

Based upon this, it was decided to conduct some preliminary experiments using the Cuming FLX-1.0 flexible, magnetically-loaded silicone rubber as a core, bent into a semi-circle so its ends pointed into the body at waist level. Alternatively, it could be left planar and tangential to the body. In its bent configuration, the gain increased by 1.9 dB at 59 MHz as compared to when the core was straight, indicating the value of using this technique to improve the amount of flux flowing through the body and the system's radiation efficiency. This experiment was repeated using the 20 turn coil on the Amidon #2 semi-circular iron powder form shown in Figure 4.2-3 and the gain increased by 4.2 dB.

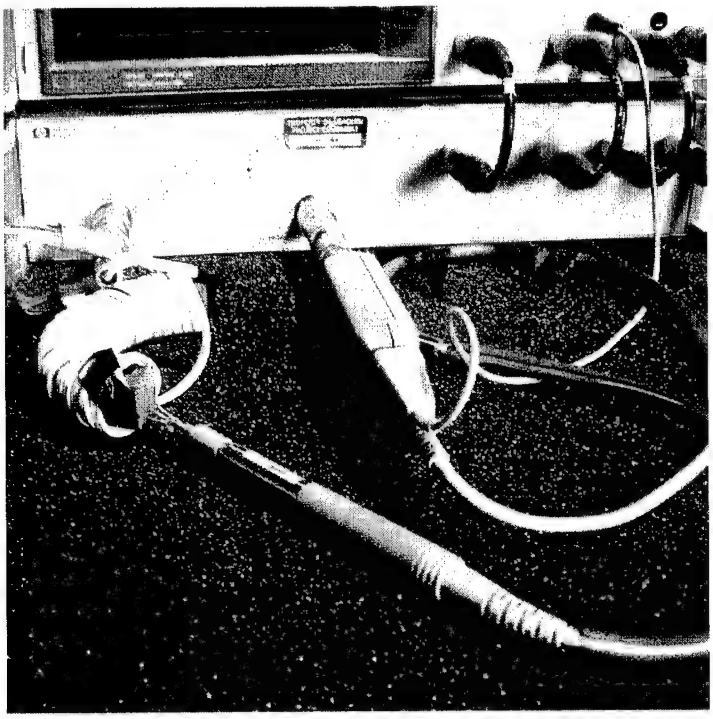

Figure 4.2-3 Test set-up used to measure relative magnetic field strength

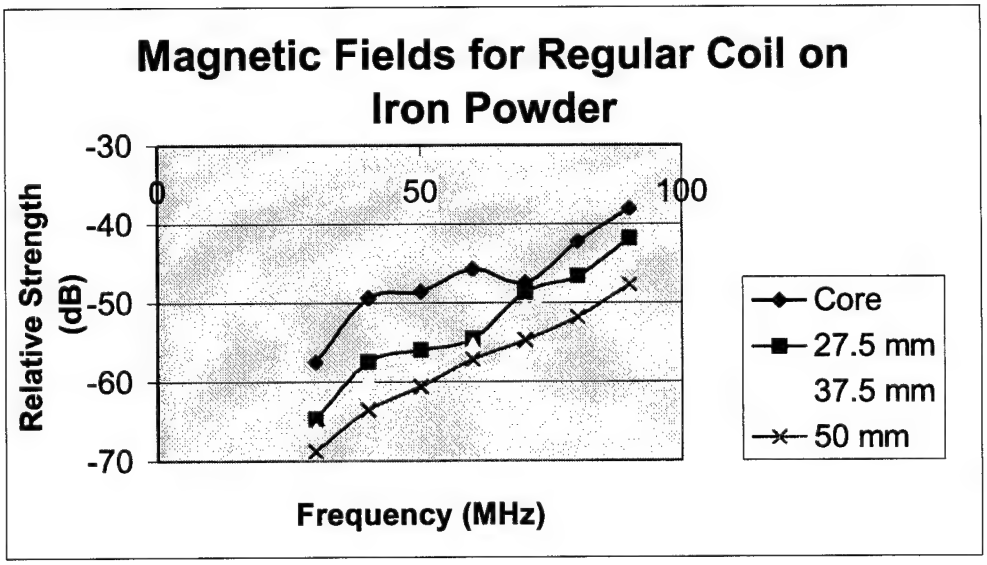

Figure 4.2-4 Relative magnetic field strength versus radial distance from core's center

4.2.3 Tesla Configured (Series Connected, Bifilar-Wound) Loops

Computations and additional preliminary experiments were conducted in order to evaluate the effect on gain and bandwidth when the helical coils were wound in a Tesla-series connected bifilar rather than the conventional single winding configuration. Figure 4.2-5 shows conventional and Tesla wound coils each with 6 turns (equal conductor lengths). The Tesla configuration consists of a bifilar, or double, winding in which the end of the first winding is connected in series to the beginning of the second winding. Tesla's theory is that if two coils of equal dimensions and 6 turns have 60 volts placed across them, the single coil will have 60/6 or 10 volts between turns and the bifilar coil 60/2 or 30 volts between turns. Since the energy stored in the coils is proportional to the square of the voltages between the turns, the energy stored in the bifilar design will be 900/100 or 9 times that of a conventionally wound coil.

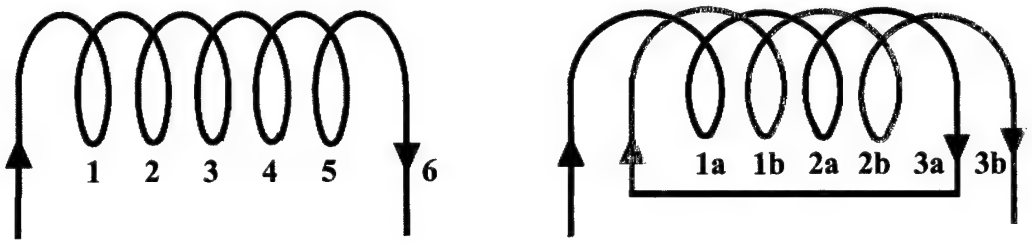

6 Turn Conventionally Wound Helical Coil

6 Turn Tesla Wound Coil

- **3 turns per winding**
- **Same length of wire as conventional coil of same number of turns**

Figure 4.2-5 Comparison of winding configurations for conventionally and Tesla wound coils of the same number of turns

Normally coils, used as inductors or H-field loop antennas are operated at 80% or less of the coil's first self-resonant frequency (SRF) where they are characterized as having an inductive reactance. Between the first and second SRFs, a conventionally wound coil exhibits capacitive reactance but still produces magnetic flux. Since we are concerned here with using the coil as a loop antenna, the sign of its feed point reactance is unimportant. Calculations and measurements for 7 turns of #16 insulated wire on a 4.8 cm diameter, 2 mm wall thickness PVC pipe, both conventionally and Tesla wound, indicated the following over the 30-88 MHz band of interest: when operated above its first SRF, the Tesla configuration had a much lower insertion loss and nearly constant ratio between its reactance and resistance ("Q") over nearly one octave. The former indicates higher efficiency, the latter a wider bandwidth as compared with conventional windings. These trends were also apparent when the Amidon #2 iron powder core of 25 x 20 mm cross section was placed in the center of the conventionally and then Tesla wound coils as shown in Figure 4.2-6, which also indicates that a Tesla configuration generates a much greater flux than a conventionally wound coil.

Experiments using different iron powder and ferrite cores, both rigid and flexible were conducted with the result that in every case, the Tesla series bifilar wound loops greatly outperformed conventionally wound ones in the three critical areas of concern: impedance, bandwidth and efficiency, especially when operated above the Tesla coils' first SRF.

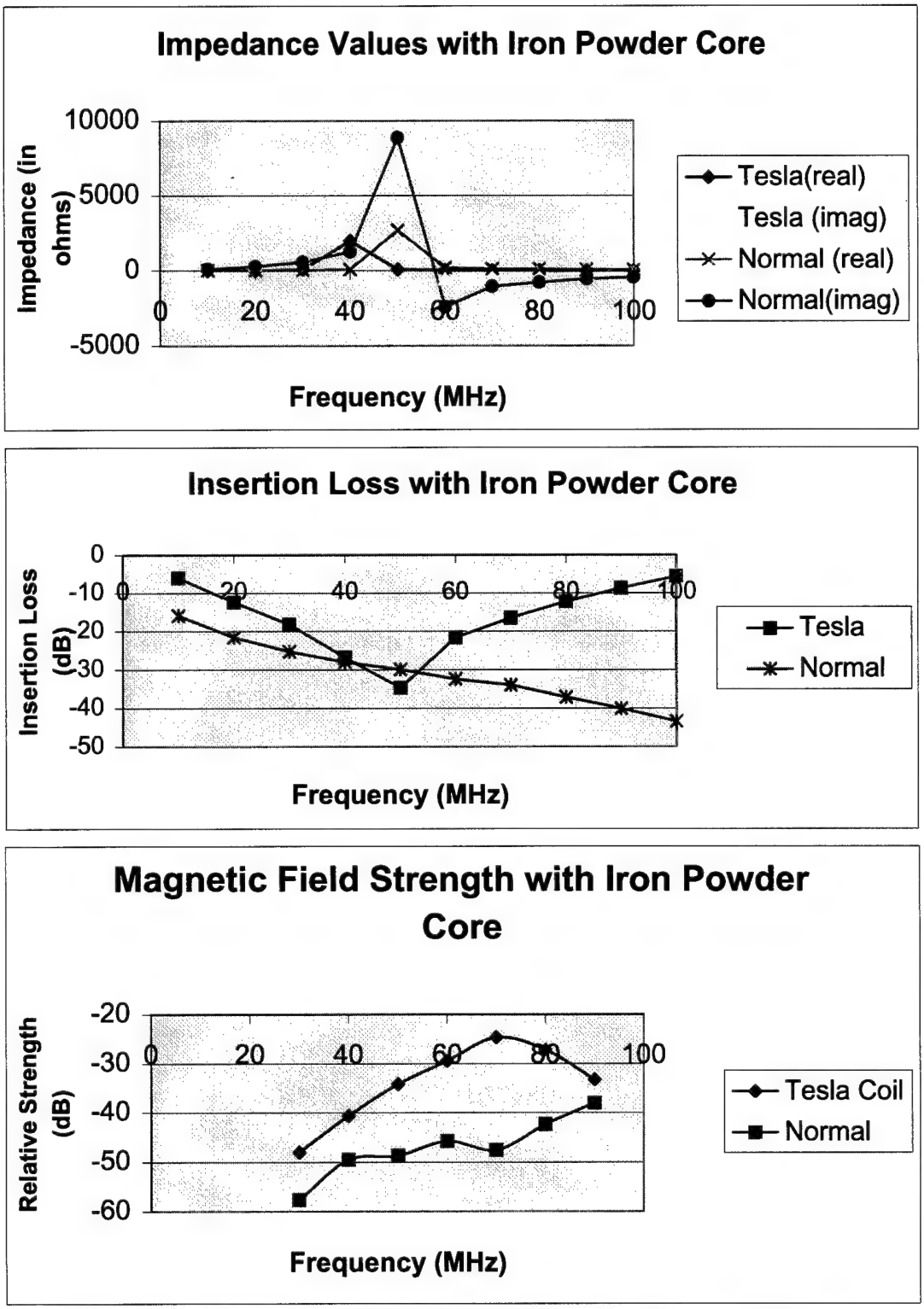

Figure 4.2-6 Characteristics of Tesla and normally-wound loops on a magnetic core

4.2.4 Multiple Critically Coupled Tesla Wound Loops

Even though we have both predicted and measured bandwidths just under one octave for Tesla series wound loops, continuous coverage across the 30-88 MHz band (1.5 octaves) without active tuning requires an impedance capable of being matched to 50 ohms with a simple, passive LC matching network or broadband impedance transformer. We performed some initial experiments to analyze the effect on bandwidth and efficiency of using multiple, critically-coupled Tesla windings of different and unequal numbers of turns around a common core. One configuration that was constructed and measured in the laboratory is shown in Figure 4.2-7. Initial results have been encouraging in that: (1) they indicate an unmatched VSWR for the configuration shown in Figure 4.2-7 of approximately 5:1 over the 30-88 MHz band, which exceeds that predicted in the literature [20] for coupled coils of equal turns and (2) the 5:1 VSWR can be matched to the required 2.5:1 or less value using a straightforward LC circuit.

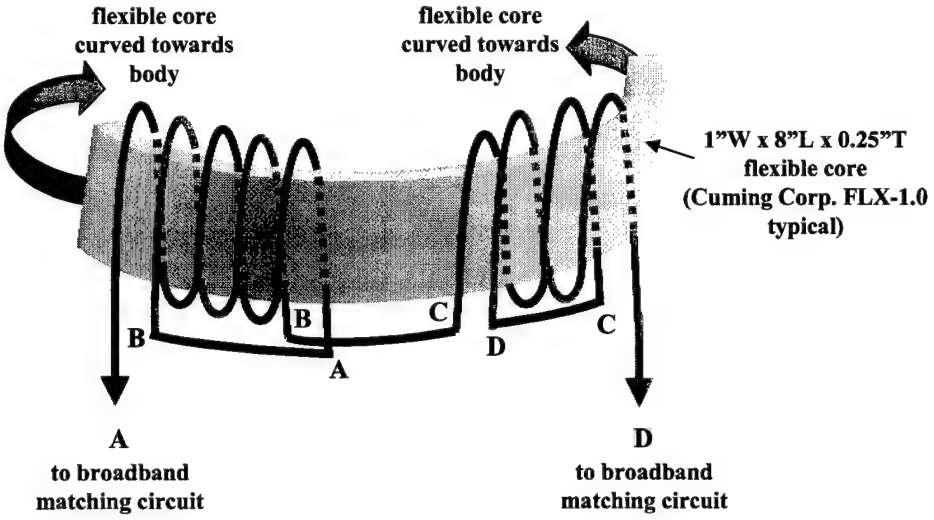

Figure 4.2-7 Experimental 30-88MHz body-coupled loop

4.3 1755-2500 MHz Enhanced Surfacewave, Body-Worn Antennas

The computations were conducted for simplicity at a frequency of 3GHz where the wavelength is 0.1m so the dimensions can easily be scaled to the other bands of interest (by multiplying by a factor of 1.7 for the 1750MHz band and 1.2 for the 2400MHz band).

Initial calculations were made using NEC-4 for the pin bed structure that was shown in Figure 3-1(a). The vertical E-field, E_z was first computed for a short dipole elevated 0.03" above a dielectric half space of ε_r=4. The input power was also noted. A 4"x4" conducting ground screen was then added to

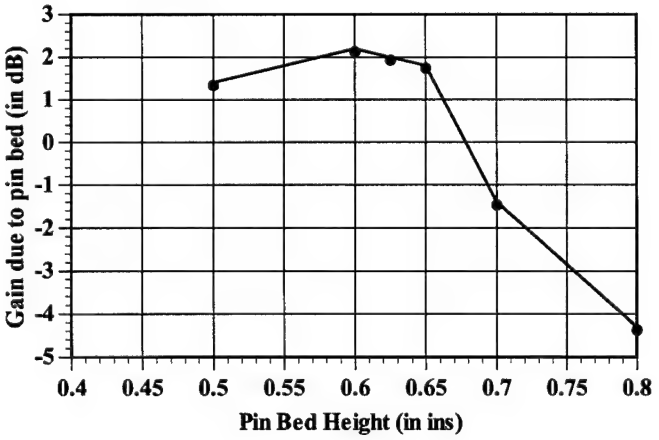

Figure 4.3-1 Change in fields due to pin bed as calculated by NEC-4

the model at the air-earth interface using a grid of wires. The fields were recomputed, and compared to those with no ground screen, taking into account the change in the input power level to the short dipole. The increase due to the conducting ground screen was determined to be 3.5dB which is consistent with other results published by Wait [6]. Vertical pins were then added to the model. The pin height was varied and the vertical E-field and input power to the dipole computed. The change in the fields due to the pin bed were then calculated again taking into account any change in the input power level. The results are plotted in Figure 4.3-1. As the pin height was varied the source dipole was moved so that its lower end was level with the top of the pin bed.

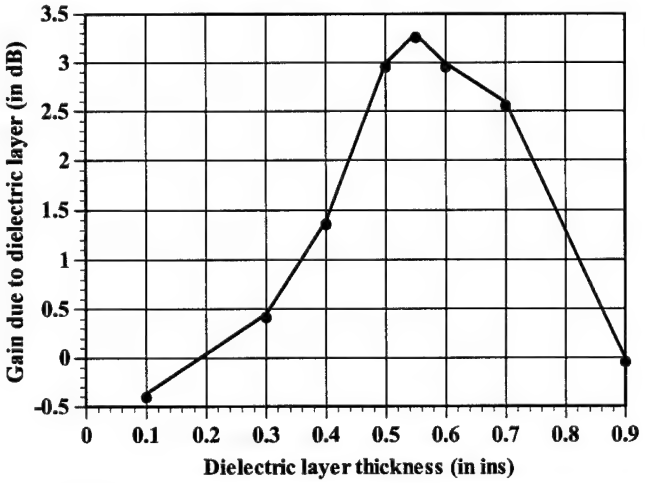

Figure 4.3-2 Change in fields due to dielectric covered ground screen as computed by XFDTD

Similar cases were run using the Finite Difference Time Domain Code XFDTD for the dielectric layer case. XFDTD was used since NEC cannot handle dielectric slabs of finite constraint. Again the fields and input powers to a short dipole were computed and compared with the no-dielectric case. The results are summarized in Figure 4.3-2. The increase in field due to introducing a conducting ground plane was again found to be 3.5dB.

It can be seen from Figures 4.3-1 and 4.3-2 that the computed increase with either the pin bed or the dielectric layer is maximum where the pin bed or dielectric thickness is approximately a quarterwave thick and is on the order of 3dB.

With the Wait analysis implemented in MathCAD, an initial check was made on the increase in gain due to introducing a 4" diameter conducting ground plane compared to no ground plane. This was determined to be 3.5dB and therefore agrees with the calculations made with NEC and XFDTD.

Other results obtained using Wait's method are shown in Figures 4.3-3 to 4.3-7. These figures show the following:

- Figure 4.3-3 shows the change in gain at 1° elevation over that of a 4" diameter perfectly conducting ground screen for a pin bed structure with the dimensions shown as a function of pin bed thickness for various dielectrics surrounding the pins, with a dielectric constant for the lower medium of 4.
- Figure 4.3-4 shows the change in gain as a function of pin height with the pins embedded in air as a function of the dielectric constant of the lower medium. This and the graph in Figure 4.3-3 show selected results for a particular set of dimensions (pin separation = 0.25", pin diameter = 0.05") for which certain approximations in the analysis are valid.
- Figure 4.3-5 shows the change in gain at 1° elevation over that of a 4" diameter perfectly conducting ground screen for a dielectric layer as a function of dielectric layer thickness for various dielectric constants, with a dielectric constant for the lower medium of 4.
- Figure 4.3-6 shows the change in gain as a function of dielectric layer thickness for a dielectric constant of the layer of 4, as a function of the dielectric constant of the lower medium.
- Figure 4.3-7 shows the difference in gain enhancement with 2", 6" and 20" diameter ground screens compared to the 4" diameter screen for the pin bed in air configuration and a lower medium dielectric constant of 4.

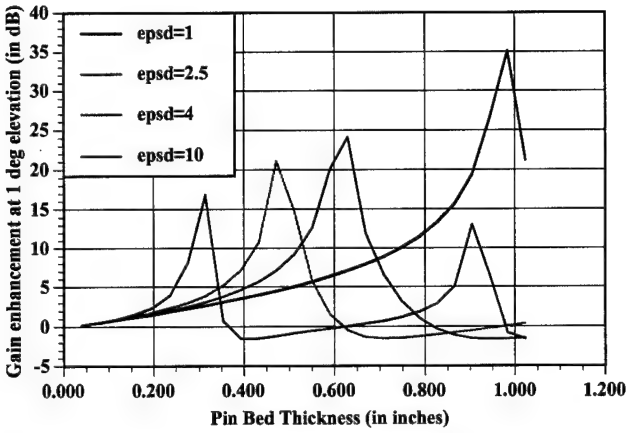

Figure 4.3-3 Computed gain enhancement with pin bed compared to ground screen only as a function of pin bed dielectric constant
Screen diameter = 4", ε_1=4.0, σ_1=0.0

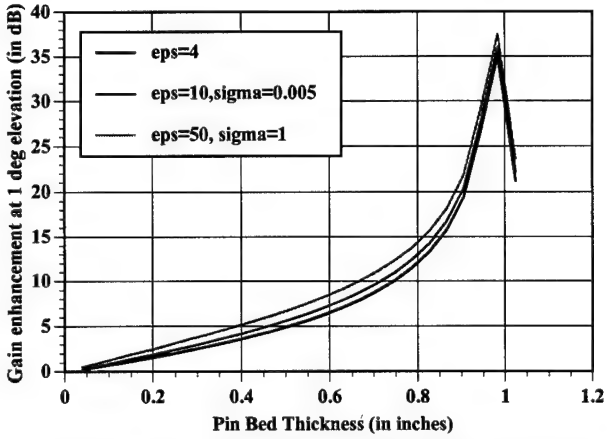

Figure 4.3-4 Computed gain enhancement with pin bed compared to ground screen only as a function of lower medium dielectric constant
Screen diameter = 4", ε_d=1.0

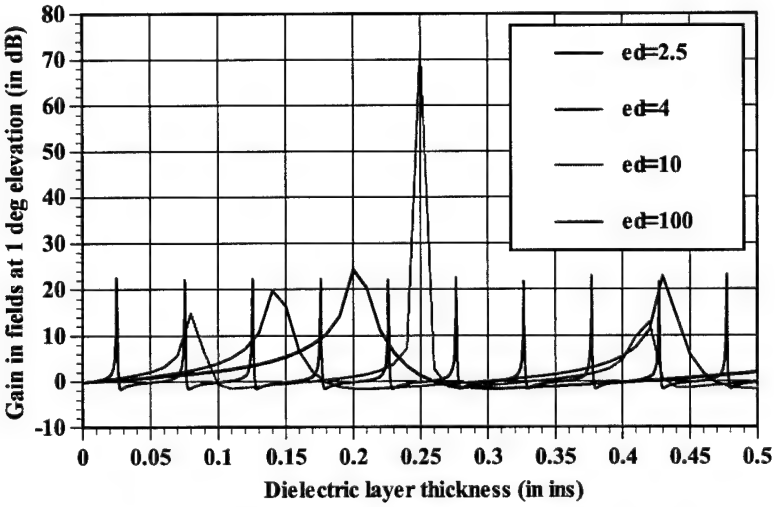

Figure 4.3-5 Computed gain enhancement with dielectric layer compared to ground screen only as a function of layer dielectric constant
Screen diameter = 4", ε_1=4.0, σ_1=0.0

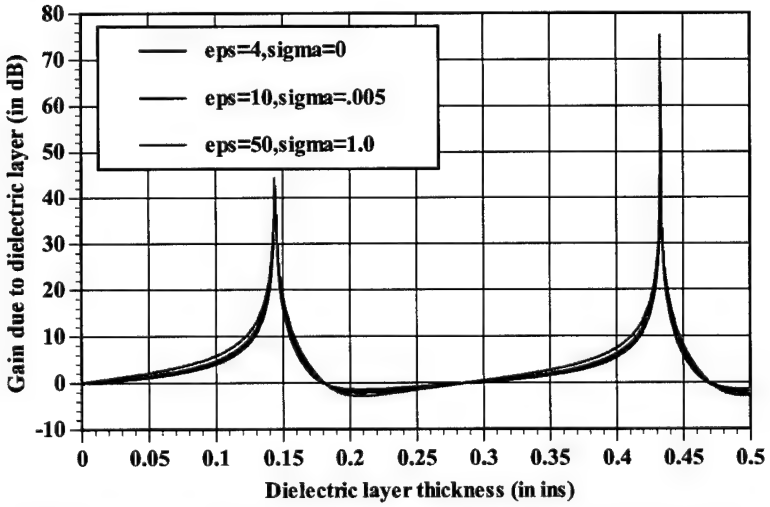

Figure 4.3-6 Computed gain enhancement with dielectric layer compared to ground screen only as a function of lower medium dielectric constant
Screen diameter = 4", ε_d=4.0

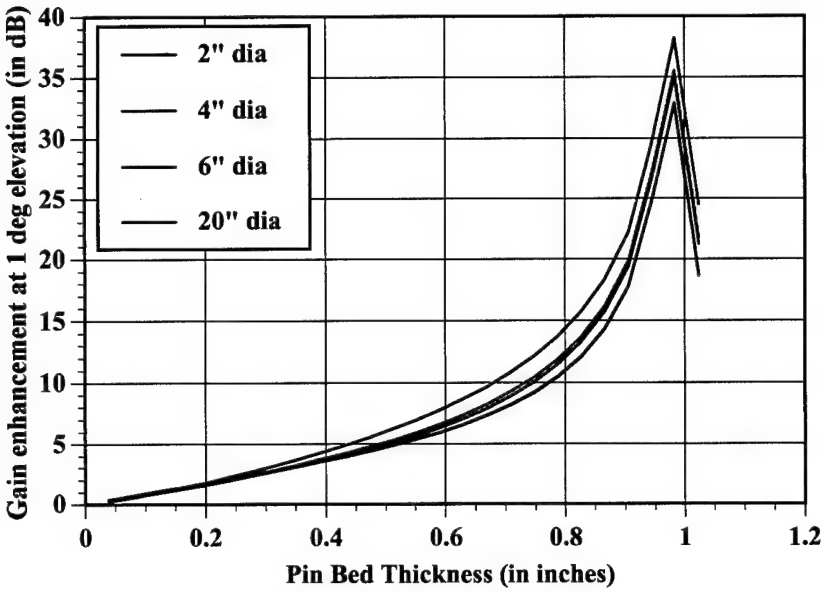

Figure 4.3-7 Computed gain enhancement with pin bed compared to ground screen only as a function of ground screen radius

ε_d=1.0, ε_1=4.0, σ_1=0.0

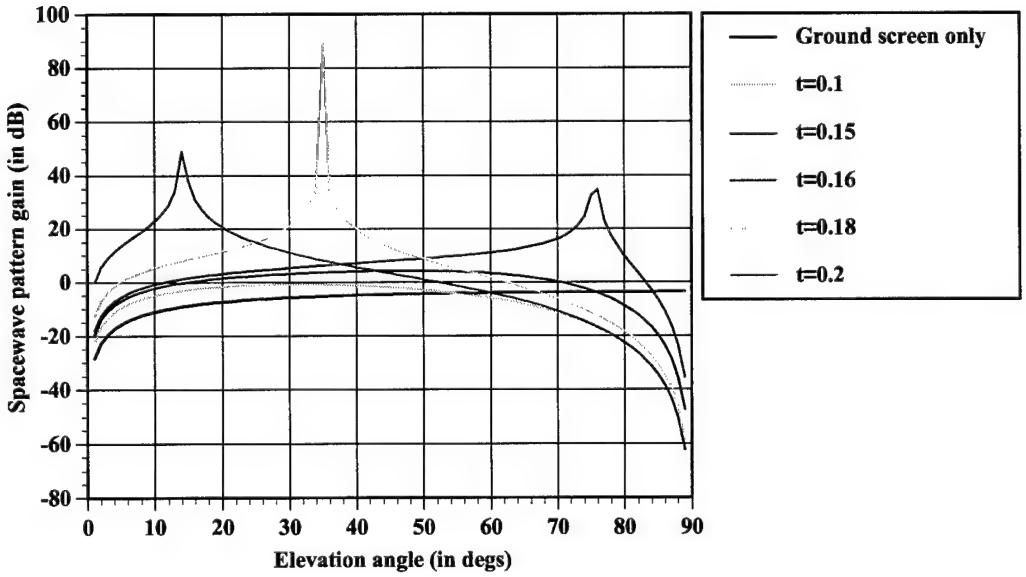

Figure 4.3-8 Computed elevation patterns with dielectric layer on ground screen as a function of dielectric thickness

ε_d=2.5, ε_1=4.0, σ_1=0.0, ground screen diameter = 4"

These figures show the following key results:

- There is a significant increase in the gain as the thickness of the pin bed approaches a quarterwave in the dielectric medium in which the pins are embedded. This can be attributed to the tangent function in equations included in Section 3.
- The magnitude of the gain enhancement decreases with increasing dielectric constant of the medium in which the pins are embedded, however, as the dielectric constant increases, the physical thickness of the pin bed decreases making it easier to accommodate on the soldier.
- The increase in gain is not highly dependent on the dielectric constant and conductivity of the lower medium.
- Increasing the ground plane size does not result in a significant change.

The analysis was then extended to include the computation of radiation pattern in the upper half space with the pin bed or dielectric layer in place (see MathCAD document in Appendix C). Figure 4.3-8 shows the computed elevation patterns for the dielectric layer case for several different thicknesses compared to the perfect ground screen case. It is seen that as the thickness of the dielectric layer increases, there is a significant enhancement in the gain at certain angles. The enhancement in the radiation pattern first appears at high elevation angles. The peak moves down in elevation angle as the thickness of the dielectric layer is increased.

The NEC-4 (pin bed) and XFDTD (dielectric layer) results also showed an increase in the fields near the air dielectric interface. However, the magnitude of the increase compared to the perfect ground screen case was only on the order of 3dB as opposed to the large increases shown by the Wait analysis. There are several possible reasons for this:

- As found in other cases, NEC does not always correctly model the fields near the air-earth interface. XFDTD may have similar limitations.
- It is known that NEC does not model diffraction effects.
- Some assumptions made by Wait and Monteath in simplifying their analysis to obtain an analytically soluble expression may need to be reviewed to ensure their validity for the cases examined here.

Considering the differences between the NEC/XFDTD and MathCAD results, a crude experimental test set-up was devised and fabricated in the laboratory using both dielectric slabs and a pin bed structure of similar dimensions to those used in the computations. One test fixture consisted of a quarterwave monopole mounted in the center of a 5 inch diameter metal ground plane. Half inch thick dielectric rings that could be placed on the ground plane having dielectric constants of 2.8 and 4.4 were also fabricated. In each case the inner radius of the dielectric ring was such as to give a 0.5 inch clearance around the base of the monopole. A second fixture with a ½ inch high grid of 0.04" diameter pins placed approximately 0.25" apart in both the x and y directions was also fabricated as shown in Figure 4.3-9. In the measurement set-up, port 1

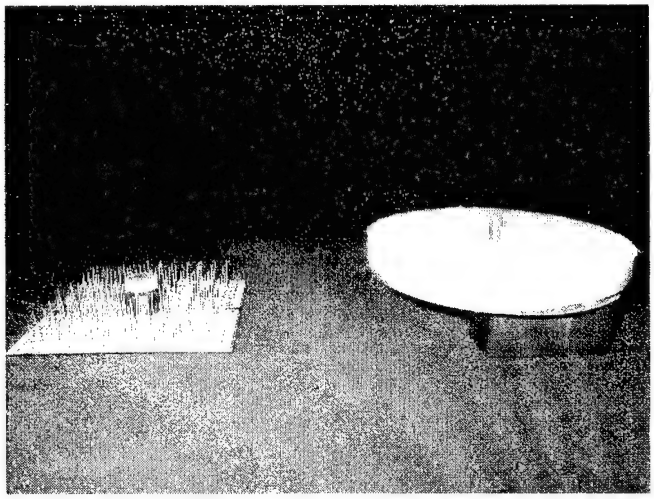

Figure 4.3-9 Preliminary pin bed and dielectric layer test fixtures

of the HP-8753C Network Analyzer was connected to the source monopole at the center of the ground plane and port 2 of the analyzer was connected to the HP-85024A high impedance probe. The field at the edge of the ground plane was measured with just the ground plane, with the various dielectric rings in place and then for the pinned structure. No second medium was used in these measurements. The results showed approximately a 2.8 and 7.6dB increase for the two dielectrics respectively and 9.8dB increase for the pin bed structure. The ½ inch thick dielectric or pin bed height corresponds to 0.127 wavelengths in free space at 3000 MHz. Using the MathCAD documents, Wait's results for similar cases showed a 6dB and 16dB increase for the two dielectrics and an 8dB increase for the pin bed case. While the results do not agree exactly, the preliminary experiment does indeed confirm that the rough order of magnitude of the increase is greater than that predicted by NEC or XFDTD and is more consistent in magnitude with that given by Wait's method.

As an offshoot from the pin bed analysis, another significant result was found – a reduced SAR antenna configuration. Initially, NEC modeling was carried out loading half the ground screen with pins and comparing the field radiated in the no pin direction with that in the direction of the pins. An apparent large increase in the fields in the pin direction was observed at some pin heights. However, when further calculations at other pin heights showed a large increase in the fields in the no pin direction, the interpretation of the results was reconsidered. It was then realized that this effect is not an enhancement in the surfacewave fields but rather a director/reflector effect due to scattering from the pins. It was ultimately found that a single row of pins would produce the same effect. A reduced SAR antenna was therefore created. Not only is there a significant null in the pin direction in the far field of the antenna but also in the near field which can be directed towards the soldier's head. The computed near field azimuth and elevation patterns are shown in Figures 4.3-10 and 4.3 -11 compared to that of the same vertical antenna with no pins. The patterns show that the fields are significantly reduced at all angles in the head direction (azimuth angle = 90°). Locating two such antennas, one on each shoulder and feeding them in phase only increases the fields in the head area by 3dB over those due to a single antenna, still resulting in a reduction of ~9dB relative to a vertical antenna on a ground screen of the same size. This result is significant and could be combined with the artificial ground plane approach to produce a low SAR, enhanced surfacewave antenna.

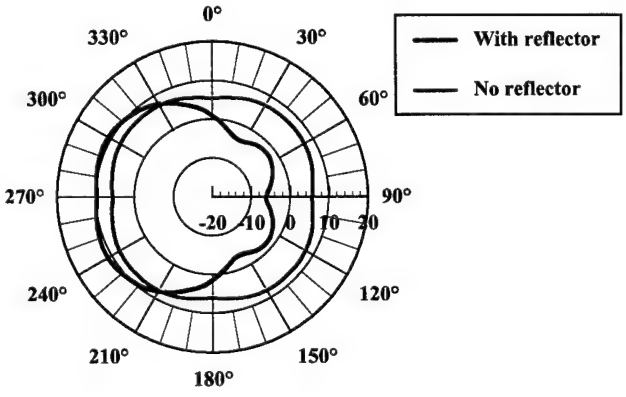

Figure 4.3-10 Computed relative near field azimuth pattern of reduced SAR antenna

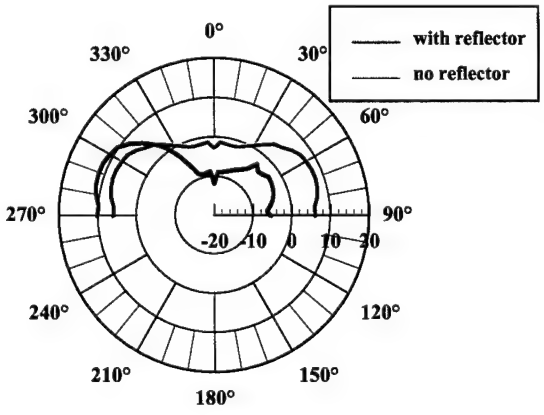

Figure 4.3-11 Computed relative near field elevation pattern of reduced SAR antenna

4.4 Switching Techniques for 1755-2500 MHz Antenna Elements

Soldier position-independent (standing to prone) radiation in the 1755-2500 MHz band will require some type of gravity actuated/controlled RF switching between various antenna elements and the soldier radio transceiver. These same switches could also be used to produce a steerable azimuthal pattern by selection of the proper elements determined by some measure of received signal quality or desired directivity provided by the soldier radio and/or GPS receivers respectively.

As part of our Phase I work, the availability, electrical performance and physical characteristics of miniature gravity actuated position sensors/switches were identified and evaluated with regard to their overall suitability for the conformal antenna suite. The envisioned suite will be comprised of: the actual enhanced surfacewave elements probably located in the vicinity on the soldier's shoulders, miniature coaxial cables and the switches themselves. It remains to be determined as to the optimum topology these three components will assume when they are attached to or sewn into the soldier's wearable equipment, (such as the MOLLE).

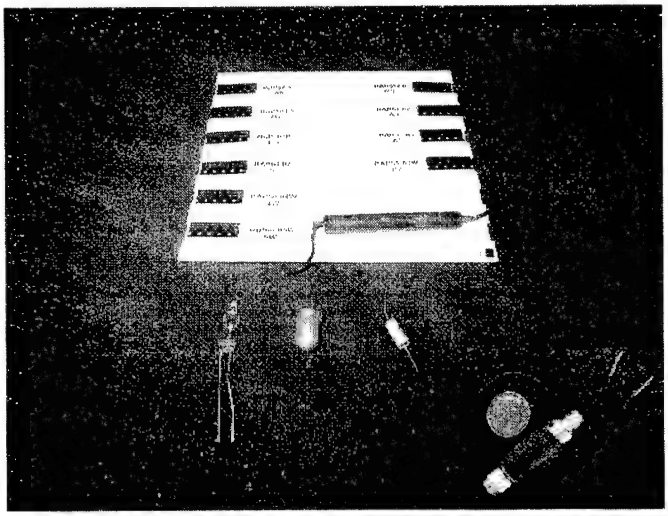

Figure 4.4-1 Switch and sensor devices evaluated in Phase I

With respect to required performance, an ideal switch will, across the band of interest; have a zero "on" and an infinite "off" impedance; low return loss; consume little power to actuate and be small, light and sufficiently robust to allow integration into the soldier worn equipment. We examined two possible schemes:

- Gravity actuated tilt switches: roller-ball, mercury and moving magnet/reed relays.
- Separate gravity actuated switches (as above) controlling remote or collocated RF switches: PIN diode, GaAs FET/MMIC or miniature mechanical latching relays via direct current control voltages multiplexed along the coaxial cables using direct current/RF isolation circuits.

Some of these are shown in Figure 4.4-1.

The first category were found to perform satisfactorily only up to approximately 400 MHz in terms of their ability to act as RF switches after measuring their "on" (insertion loss), "off" (isolation) and return loss (VSWR) characteristics with the HP-8753C Vector Network Analyzer. The mercury switches had an excessive "on" insertion loss due to the fact that mercury is a poor RF conductor at microwave frequencies. In addition, the roller-ball "tilt" switches were found to have unacceptable levels of "contact-bounce" even with slight movement.

The suitability of several alternative switches listed in the second category was evaluated by reviewing manufacturers' specifications and application notes. The most promising of each currently appear to be available from: Philips (BAP series of SMD PIN diodes [21]), MCL (RSW FET/MMIC with integrated TTL driver [22]) and MicroNetics (MSM1 series of electro-mechanical miniature relays [23]). Of these, PIN diodes appear to offer the best off-the-shelf performance: reasonable insertion loss (0.5dB); better than 30 dB of isolation; less than 1.2 VSWR; low power consumption (10 mW or less); and the ability to easily handle the soldier radio's output power. PIN diodes however cause intermodulation (IM) products which may or may not be important here.

One very promising category of RF switches are MEMS electromechanical relays being developed by companies/universities such as: Dow-Key Microwave/Microlab/ASU, Integrated Micro Machines, HRL Laboratories, Analog Devices/NU, Cronos Integrated Microsystems and UCLA. The existing Dow-Key die is 2x3 mm, has less than 0.1 dB insertion loss and 40 dB isolation at 1755 MHz, can handle 2.5 watts and a measured IMD of –85 dBc [27]. Since it is a latching (bi-stable) design, it consumes no power in its quiescent state and only 40 microjoules to throw it from one SPDT state to the other. A fully protected "capped" version will be available in 2002.

5.0 Conclusions

Based upon our work during the past six months, the results of which are summarized in the previous section, we have concluded the following regarding technical feasibility and risk for each of the three major portions of our research:

- **30-88 MHz Body-Coupled, Multiple, Tesla Series Wound, Magnetically-Loaded Helical Loop Antennas**
  By combining these four techniques it is likely that a practical antenna meeting the performance goals stated in Section 4.1 will be possible, with only moderate risk, to be fabricated, tested and demonstrated during any Phase II effort. The majority of the risk associated with this antenna is in finding a suitable (low loss factor) flexible magnetic core material. This conclusion is supported by the literature, some calculations and a number of laboratory experiments that clearly indicate that: when excited by a small loop antenna whose axis is orthogonal to the torso the human body becomes an efficient antenna at low VHF; Tesla wound coils produce greater flux over much wider bandwidths than conventionally wound coils; this flux can be guided into the human body using flexible magnetic cores and additional bandwidth can be obtained by placing several, critically coupled unequal Tesla windings on a common core.

- **1755-2500 MHz Enhanced Surfacewave, Body-Worn Antennas**
  The major conclusion that can be drawn from our Phase I work is that an enhancement in the surfacewave fields is possible with a thin (<0.5") pin bed or dielectric structure on a small ground screen on the order of a few inches square. The thickness can be traded against the dielectric constant of the material in which the pins are embedded or of the dielectric layer. This conclusion was supported both by theory and preliminary experiments.

  The several analytical techniques used to model the pin bed and the dielectric layer produced differing results. Wait's method showed a significant (10's of dB's) improvement in the fields when the thickness of the dielectric layer or the pin bed is a quarterwave in the dielectric. By contrast, NEC-4 and XFDTD showed an improvement of only ~3dB when NEC-4 was used to model the pin bed and XFDTD was used to model the dielectric layer. However, a preliminary experiment conducted using a pin bed and two dielectrics of differing dielectric constants showed increases in the field levels similar to those predicted by Wait. It was therefore concluded that a large enhancement is indeed possible. That such an effect exists, is supported by other articles in the open literature. Similar large increases in gain have been documented using periodic structures. For example, Yang et al [24] showed significant increases at certain elevation angles for a horizontal Hertzian dipole lying on a periodic photonic bandgap structure. It can be concluded therefore, that this type of enhancement is realizable.

As described Wait's method was implemented for a uniform ground plane i.e. the ground plane had the same surface impedance as a function of the radial distance from the source and as a function of azimuthal angle ϕ. The reason for considering this case is that Wait's integral in the MathCAD document becomes simpler to evaluate. The elevation patterns were shown to produce a large value at certain angles over a narrow angular range for certain ground plane characteristics. It was also shown that this "spike" in the patterns moves as the ground plane properties are changed. It can therefore be concluded that the potential exists for customizing the radiation patterns solely by adjusting the ground plane impedance and that with artificial ground planes, an increased gain and therefore reduced SAR is possible. These results also indicate that there is a long term potential for adaptively changing the pattern of a body worn antenna by controlling the ground plane parameters using some form of switching.

- **Switching Techniques for the 1755-2500 MHz Antenna Elements**

We have concluded that in the near term gravity actuated position sensors controlling dispersed PIN diode RF switches using simple isolation circuits and miniature coaxial cables will be capable of being integrated into worn equipment while providing usable RF performance. However as part of our work we have become aware of the progress being made by many universities and companies in developing and marketing micro-mechanical relay MEMS latching RF switches that will offer: significant weight; size; power and RF-insertion-loss, isolation and IMD performance over the PIN diodes. The MEMS switches will be available in 2002.

6.0 Recommendations

Based upon our work described in the previous sections we recommend that the soldier conformal antenna suite be transitioned from the mostly theoretical and limited experimental efforts to a final, tested and fully characterized prototype conformal antenna suite suitable for link testing and demonstrations to government and private sector users. The following specific recommendations are included here for each of the three areas investigated: 30-88 MHz conformal body-coupled loop, 1755-2500 MHz artificial dielectric conformal ground plane antennas and switching devices for the latter.

- **30-88 MHz**

We recommend additional analysis using MathCAD to compute the free space impedance, bandwidth and gain/efficiency of candidate magnetically loaded, single and multiple helical loop designs across the 30-88 MHz band to determine the best performing (bandwidth and gain) designs in terms of: dimensions, conductor size, inter-turn spacing, winding and core geometries, core-to-winding spacing, number of separate-critically coupled common-core loops and the number of Tesla-series connected turns for each. These calculations should be based on the work of Smith [15], DeVore and Bohley [16] and Abrie [20]. The candidate designs should then be modeled when tangent to (straight core) and coupled into (bent core) the body using XFDTD to determine the amount of enhanced gain due to both conditions.

We also recommend that the above be complemented with additional laboratory and antenna range measurements once a chosen prototype loop system design is available. Figure 6-1 indicates a recommended setup to measure power gain.

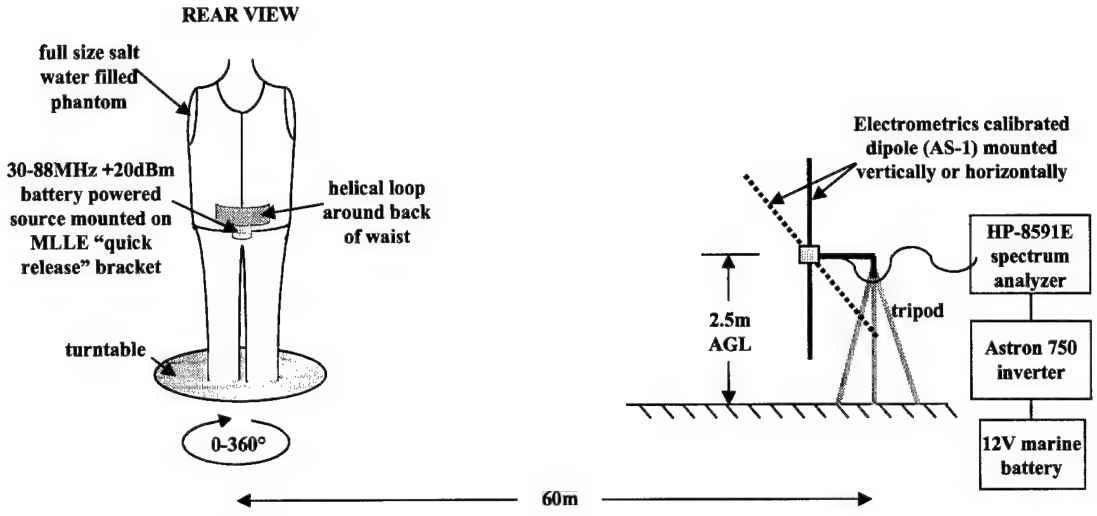

Figure 6-1 Recommended setup for measuring power gain

- **1755 to 2500 MHz**

Based on the results described in Section 4 and the conclusions presented in Section 5, several recommendations for further work are:

- Improving/reviewing the analysis techniques to understand and resolve the differences in the various computational approaches.
- Developing a definitive measurement set up for accurately determining any enhancement in the fields due to the presence of the pinned or dielectric ground planes to support the computational approach.
- Developing an analysis for artificial ground planes whose impedance characteristics vary as a function of distance from the source and with azimuth angle since it is believed that this could potentially yield significant results in terms of allowing us to tailor the radiation pattern to best fit the soldier platform.

Each of these will now be discussed in turn.

Improving/reviewing the analysis techniques

The purpose of this would be to resolve outstanding issues from Phase I regarding the differences between the NEC/XFDTD and Wait results. In principle, the NEC and XFDTD methods should yield an accurate picture of the fields since they are based on Maxwell's equations. However computer code realizations always involve some approximations that are not always apparent to the user and may give erroneous results. For example, previous experience using NEC to model buried ELF antennas showed that the magnetic field at the surface agrees with the classic Sommerfeld-Norton results only if the observing point is below the air-earth interface. During our recent work, erratic results for the field values were obtained when using the 'RP1' versus the 'NE' field computation options in NEC. The 'RP1" option supposedly provides for computation of the surface and space wave fields. The 'NE' option computes the near fields. The 'NE' results were found to be erroneous if the observation point was at the air-earth interface at z=0. Differences between the 'NE' and 'RP1' results were observed close in to the

antenna. It is likely that similar issues can arise with XFDTD due to some limitation of the code since many approximations are also used in the method. While the **E**lectromagnetic **C**ompensation **T**heorem (ECT) is quite rigorous in its basic expression as reviewed by Monteath [25], many approximations were made in reducing it to the point used by Monteath [25,26] and Wait [6]. This was done so that they were able to obtain practical formulas that could be solved analytically. One such approximation, for example, is that the tangential magnetic field on the surface of integration is assumed to be of the same structural form regardless of the actual surface under the antenna. Monteath alludes to this in his study of the effect of a perfect ground screen and argues that this field differs from his (and Wait's) only in a very small region next to the outer edge of the screen. Secondly in applying the ECT, Monteath, Wait and others assume that the tangential electric field is related to the magnetic field by a surface impedance that is independent of position on the screen, and only varies piecewise in going from one type of screen to another. An exception to this is the screen of radial wires. To understand and resolve these computational issues, so that we are able to better develop an analytical model of the geometries of interest and understand the limitations of the available analysis techniques, a review the original Monteath analysis is required, and the approximations assessed to determine any impact this may have on the MathCAD implementation.

Developing a definitive measurement set up for pinned or dielectric ground planes

The purpose of this would be to provide a test bed for evaluating the selected ground screens that result from the improved and refined analysis techniques. It is recommended that a test bed be designed, that could easily accommodate different ground screens under evaluation and that will allow the fields near the edge of the ground screen and at varying distances from the ground screen to be measured in a controlled and repeatable fashion and compared with the fields radiated by the same source antenna mounted on a conventional metallic screen. One possible test bed set up is illustrated in Figure 6-2. With a ground plane size of 4" diameter, the overall size of the outer wooden box may be on the order of 16" square and 1-2" in height.

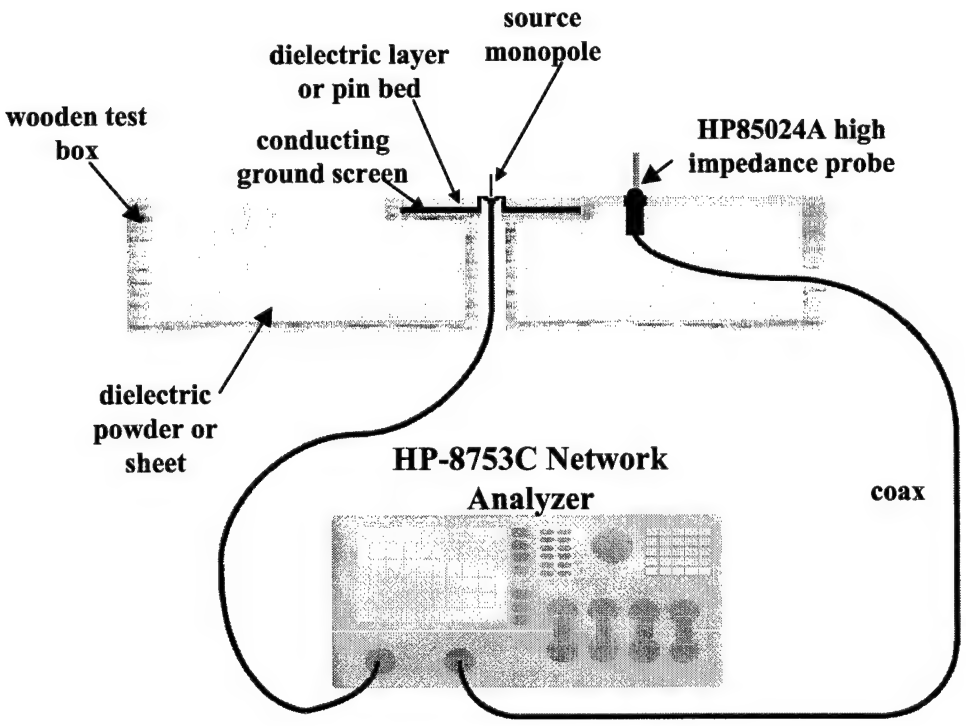

Figure 6-2 Suggested Test Bed for Evaluating Artificial Ground Screens

Complex Ground Screen Configurations

Wait ECT approach is ideally suited to the study of surfaces whose properties may be changed as a function of distance from the antenna. It is clear from equation (1) that if Z_n varies in a stepwise fashion with increasing radius from the source, then the value of Ωa can also be evaluated piecewise for each value of Z_n. In this way, it will be possible to model ground screens with non-uniform impedance characteristics. These may include both capacitive and inductive surfaces. With a dielectric layer, an inductive surface impedance is produced for all dielectric thicknesses less than a quarter wavelength in the dielectric. Either an inductive or a capacitive surface impedance can be obtained with the pin bed structure depending on the height, diameter and separation of the pins.

As an alternative to varying the surface impedance as a function of the radial distance from the source, consideration could also be given to changing the surface impedance characteristics as a function of the azimuth angle. This scenario can also be handled by Wait's method and will lead to being able to control and direct the azimuthal radiation patterns.

7.0 References

1. Cross, M.W., "Innovative Soldier Conformal Antenna Suite: Task 1 Report", Contract DAAD-16-01-C-007, 28 February, 2001.
2. Tesla, N., "Coil for Electromagnets", USP 512,340, 9 January, 1894.
3. G. J. Burke, Numerical Electromagnetics Code - NEC-4, Method of Moments, Lawrence Livermore Laboratory, January 1992.
4. Remcom Inc., XFDTD Finite Difference Time Domain Program, State College, PA.
5. MathSoft, Inc., MathCAD 2001 Professional, Cambridge, MA.
6. Wait, J.R., "On the theory of radiation from a raised electric dipole over an inhomogeneous ground plane" Radio Science, Vol.2, pp. 997-1004, 1967.
7. King, R.J., Thiel, D.V. and Park, K.S., "The synthesis of surface reactance using an artificial dielectric". IEEE Transactions on Antennas and Propagation, Vol.AP-31, No. 3, May 1983.
8. Andersen, J.B. and Hansen, F., "Antennas for VHF/UHF Personal Radio: A Theoretical and Experimental Study of Characteristics and Performance", IEEE Trans. Veh. Tech., Vol. VT-26, No. 4, November, 1977.
9. Krupka, Z., "The Effect of the Human Body on Radiation Properties of Small-Sized Communication Systems", IEEE Trans. Ant.& Prop., Vol. AP-16, No. 2, March, 1968.
10. Chen, W.T. and Chuang, H.R., "Numerical Computation of Human Interaction with Arbitrarily Oriented Superquadric Loop Antennas in Personal Communications", IEEE Trans. Ant.&Prop., Vol. 46, No. 6, June, 1998.
11. King, H.E., "Characteristics of Body-Mounted Antennas for Personal Radio Sets", IEEE Trans. Ant.& Prop., pp 242-244, March, 1975.
12. Fujimoto, K., et al, "Small Antennas", Research Studies Press, UK, 1987.
13. Oleson, J.R., "A Review of Magnetic Induction Methods for Hyperthermia Treatment of Cancer", IEEE Trans. Bio. Engr., Vol. BME-31, No.1, January, 1984.
14. Ruggera, P.S. and Kantor, G., "Development of a Family of RF Helical Coil Applicators Which Produce Transversely Uniform Axially Distributed Heating in Cylindrical Fat-Muscle Phantoms", IEEE Trans. Bio. Engr., Vol. BME-31, No. 1, January, 1984.
15. Smith, G.S., "Radiation Efficiency of Electrically Small Multiturn Loop Antennas", IEEE Trans. Ant.&Prop., September, 1972.
16. DeVore, R. and Bohley, P., "The Electrically Small Magnetically Loaded Multiturn Loop Antenna", IEEE Trans. Ant.&Prop., Vol. AP-25, No. 4, July, 1977.

17. Siwiak, K., "Radiowave Propagation and Antennas for Personal Communications", Artech House, Boston, MA, 1995.
18. Padhi, T., "Theory of Coil Antennas", Radio Sci., Vol. 69D, 1965.
19. Cross, M., "Final Technical Report: Phase II High Temperature Superconducting (HTSC)-Tuned, Electrically-Small MF/HF Antenna System Design and Measured Performance", DAAB 10-94-D-0503/0064, QuesTech Subcontract # SC-1864, July, 1997.
20. Abrie, P.L.D., "The Design of Impedance Matching Networks for RF and Microwave Amplifiers", Artech House, Norwood, MA, 1985.
21. Philips Electronics N.V., PIN Diode Product Overview, 1999.
22. Mini Circuits Corp. RF/IF Designers Guide, DG-2001, Brooklyn, NY, 2001.
23. Micronetics Inc., Specification Sheet MSM1 Switch, Hudson, NH, 2001.
24. Yang, H.-Y. D., Alexopoulos, N. G. and Yablonovitch, E, "Photonic Bandgap Materials for High Gain Printed Circuit Antennas", IEEE Trans. on Antennas and Propagation, Vol. AP-45, No. 1, January 1997, pp. 185-186.
25. Monteath, G.D., "Application of the compensation theorem to certain radiation and propagation problems" Proceedings of the Institution of Electrical Engineers (London), Vol.98, Part IV, Monograph No.3, 1951.
26. Monteath, G.D., "The effect of the ground constants and of an earth system on the performance of a vertical medium-wave aerial" Proceedings of the IEE (London), Monograph 279R, pp. 292-306, January 1958.
27. Campbell, T., "MEMS Switch Technology Approaches the Ideal Switch", Applied Microwave and Wireless Magazine, pp. 100-107, May 2001.

APPENDIX A:

This MathCAD document row_pin-bed.mcd allows the computation of the gain in the fields at a 1 deg elevation angle for a pin bed ground screen. The top of the layer is level with the bare earth. Wait's theory is used. The thickness of the pin bed is incremented. The dielectric constant of the material in which the pins are embedded can also be changed (EPSd).

The integrals defined by Wait are evaluated for effect on the low angle fields for a circular ground screen of a given surface impedance. The antenna height h cannot be equal to zero.

$f := 3.0 \cdot 10^9$ frequency in Hz $\lambda 0 := \frac{2.9979610^8}{f}$ $\lambda 0 = 0.099932$ wavelength

$s := 0.0508$ radius of ground screen in meters (set to 2")

$k := 2 \cdot \frac{\pi}{\lambda 0}$ $k = 62.87461$ propagation constant in free space

$ks := \frac{2 \cdot \pi}{\lambda 0} \cdot s$ $ks = 3.19403$

$\Psi\Psi := 1.0$ elevation angle of observer in degrees

$\Psi := \Psi\Psi \cdot \frac{\pi}{180}$ elevation angle in radians

$v := \cos(\Psi)$

$h := 0.000254$ height of antenna above perfectly conducting scree and dielectric surface

$\delta t := 0.01 \cdot \lambda 0$ increment for dielectric layer thickness

$n := 0, 1 .. 50$ number of increments in the layer thickness

$t_n := n \cdot \delta t$ thickness of the layer over the perfect ground screen $w := h \cdot k$

Note: w cannot be set to zero in the integral I2 below

$F(u) := e^{\left(-i \cdot \sqrt{u^2+w^2}\right)} \cdot J1(u \cdot v) \cdot \left(\frac{u^2}{u^2+w^2}\right)$ Evaluate Wait's integral by parts

$I1 := \int_0^{ks} F(u)\, du$

$I2 := \left(\frac{1}{i}\right) \cdot \int_0^{ks} \left(\frac{1}{u}\right) \cdot F(u)\, du$

$I := I1 + I2$

$\Omega n := \left(\frac{1}{v}\right) \cdot I$ $\Omega n = -0.90879 - 1.22273i$

Bare earth properties: $EPS := 4$ dielectric constant $SIGMA := 0$ conductivity

$nn := EPS - i \cdot 1.7975510^{10} \cdot \frac{SIGMA}{f}$ $nn = 4$ refractive index of earth squared

$ZNORM0 := \frac{\sqrt{\left(nn - \cos(\Psi)^2\right)}}{nn}$ normalized surface impedance of the bare earth

$Rv0 := \frac{\sin(\Psi) - ZNORM0}{\sin(\Psi) + ZNORM0}$ reflection coefficient from bare earth at antenna height h

$G0h := \frac{e^{i \cdot k \cdot h \cdot \sin(\Psi)} + Rv0 \cdot e^{-i \cdot k \cdot h \cdot \sin(\Psi)}}{1 + Rv0}$

$\Omega a := \Omega n \cdot (-ZNORM0)$ $\Omega a = 0.39354 + 0.52948i$

is the gain factor for a perfectly conducting circular ground screen with the antenna at its given height. If it is << Goh then the screen has a small effect on the field strength. If it is >> Goh then the screen has a significant effect.

$Wprime := (1 + Rv0) \cdot \frac{G0h + \Omega a}{2}$ $|Wprime| = 0.05785$ no ground screen present

$Wprime0 := (1 + Rv0) \cdot \frac{G0h}{2}$ $|Wprime0| = 0.03874$ with perfect ground screen

$G := 20 \log\left(\left|\frac{Wprime}{Wprime0}\right|\right)$ $G = 3.4822$ dB field strength improvement in dB with perfect ground screen and antenna at its minimum height

---

Ground screen gain with bed of pins structure:

$a := 0.00635$ Pin bed dimensions: a,b = x and y direction spacing, d=pin diameter

$b := 0.00635$

$d := 0.00127$

$A := \frac{\pi \cdot a}{\left(b \cdot \ln\left(\frac{b}{\pi \cdot d}\right)\right)}$ $A = 6.76036$

$EPSd := 1$ dielectric constant of material surrounding pins

$kd := k \cdot \sqrt{EPSd}$ $kd = 62.87461$

$\theta := kd \cdot a$ $\theta = 0.39925$

$p := \frac{1}{\theta} \cdot \operatorname{acosh}\left(\cos(\theta) + \frac{A}{\theta} \cdot \sin(\theta)\right)$ $p = 6.77276$

Surface impedance of bed of pins computed according to King et al.

$$D := \frac{\pi \cdot d^2}{2 \cdot a^2} \qquad D = 0.06283$$

$$EPSx := EPSd \cdot \left[\frac{1 + \frac{D}{2}}{1 - \frac{D}{2}} \right] \qquad EPSx = 1.06487$$

$$kz1 := \left(kd^2 + \frac{k^2}{p^2} \right)^{.5} \qquad kz1 = 63.55626$$

$$t0 := 0.01 \cdot \lambda 0 \qquad t0 = 9.9932 \cdot 10^{-4}$$

$$\delta := 0.01 \cdot \lambda 0 \qquad \delta = 9.9932 \cdot 10^{-4}$$

$$n := 0, 1 .. 50$$

$$t_n := t0 + \delta \cdot n$$

$$X_n := kz1 \cdot \frac{\tan(kz1 \cdot t_n)}{EPSx \cdot k}$$

normalized surface reactance of the pin bed from King et al

$$Z_n := i \cdot X_n$$

normalized surface reactance of the pin bed

Ground screen gain with a pin bed structure:

$$Zaprime_n := Z_n - ZNORM0$$

$$Rv := \frac{\sin(\Psi) - ZNORM0}{\sin(\Psi) + ZNORM0}$$

reflection coefficient

$$\Omega aa_n := Zaprime_n \cdot \Omega n$$

$$Wpp_n := (1 + Rv) \cdot \frac{G0h + \Omega aa_n}{2}$$

$$Gp_n := 20 \cdot \log\left(\left| \frac{Wpp_n}{Wprime} \right| \right)$$

field strength with pin bed ground screen relative to perfectly conducting ground screen

Plot of field strength enhancement as a function of dielectric layer thickness

$s = 0.0508$ $EPS = 4$ $SIGMA = 0$ $EPSd = 1$

$h = 2.54 \cdot 10^{-4}$ height of dipole above surface

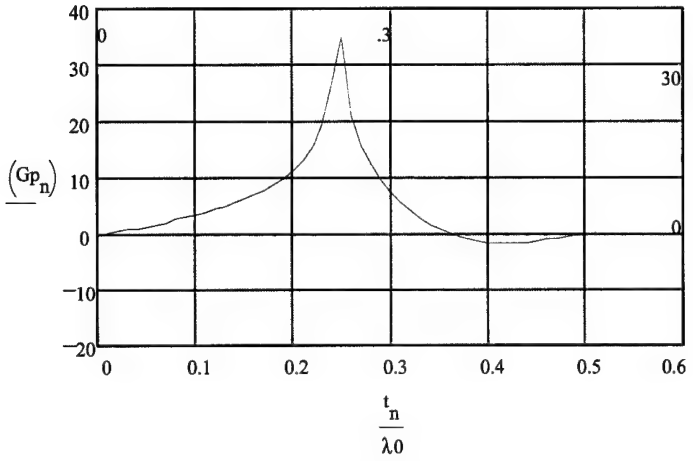

Plot of sigma as a function of dielectric layer thickness

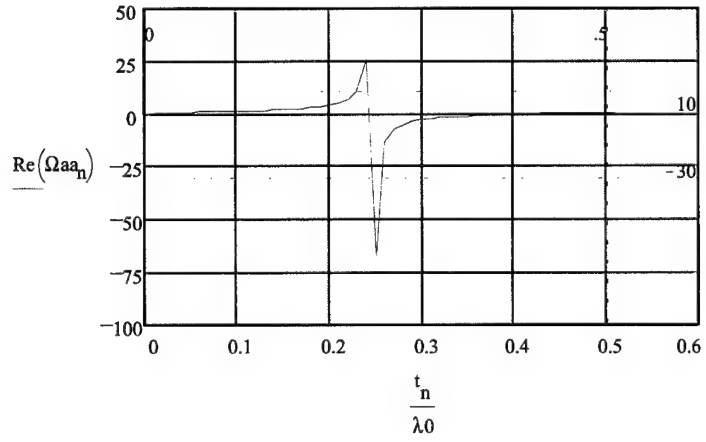

APPENDIX B

This MathCAD document row_dielectric_layer.mcd allows the computation of the gain in the fields at a 1 deg elevation angle for a dielectric covered ground screen. The top of the layer is level with the bare earth. Wait's theory is used. The thickness of the dielectric layer is incremented.

The integrals defined by Wait are evaluated for effect on the low angle fields for a circular ground screen of a given surface impedance. The antenna height h cannot be equal to zero.

$f := 3.0 \cdot 10^9$ frequency in Hz $\lambda 0 := \frac{2.9979610^8}{f}$ $\lambda 0 = 0.099932$ wavelength

$s := 0.0508$ radius of ground screen in meters (set to 2")

$k := 2 \cdot \frac{\pi}{\lambda 0}$ $k = 62.87461$ propagation constant in free space

$ks := \frac{2 \cdot \pi}{\lambda 0} \cdot s$ $ks = 3.19403$

$\Psi\Psi := 1.0$ elevation angle of observer in degrees

$\Psi := \Psi\Psi \cdot \frac{\pi}{180}$ elevation angle in radians

$v := \cos(\Psi)$

$h := 0.000254$ height of antenna above perfectly conducting scree and dielectric surface

$\delta t := 0.01 \cdot \lambda 0$ increment for dielectric layer thickness

$n := 0, 1 .. 50$ number of increments in the layer thickness

$t_n := n \cdot \delta t$ thickness of the layer over the perfect ground screen $w := h \cdot k$

Note: w cannot be set to zero in the integral I2 below

$F(u) := e^{\left(-i \cdot \sqrt{u^2+w^2}\right)} \cdot J1(u \cdot v) \cdot \left(\frac{u^2}{u^2+w^2}\right)$ Evaluate Wait's integral by parts

$I1 := \int_0^{ks} F(u)\, du$

$I2 := \left(\frac{1}{i}\right) \cdot \int_0^{ks} \left(\frac{1}{u}\right) \cdot F(u)\, du$

$I := I1 + I2$

$\Omega n := \left(\frac{1}{v}\right) \cdot I$ $\Omega n = -0.90879 - 1.22273i$

Bare earth properties: $EPS := 4$ dielectric constant $SIGMA := 0$ conductivity

$nn := EPS - i \cdot 1.7975510^{10} \cdot \frac{SIGMA}{f}$ $nn = 4$ refractive index of earth squared

$ZNORM0 := \frac{\sqrt{\left(nn - \cos(\Psi)^2\right)}}{nn}$ normalized surface impedance of the bare earth

$Rv0 := \frac{\sin(\Psi) - ZNORM0}{\sin(\Psi) + ZNORM0}$ reflection coefficient from bare earth at antenna height h

$$G0h := \frac{e^{i \cdot k \cdot h \cdot \sin(\Psi)} + Rv0 \cdot e^{-i \cdot k \cdot h \cdot \sin(\Psi)}}{1 + Rv0}$$

$\Omega a := \Omega n \cdot (-ZNORM0)$ $\Omega a = 0.39354 + 0.52948i$

is the gain factor for a perfectly conducting circular ground screen with the antenna at its given height. If it is << Goh then the screen has a small effect on the field strength. If it is >> Goh then the screen has a significant effect.

$Wprime := (1 + Rv0) \cdot \frac{G0h + \Omega a}{2}$ $|Wprime| = 0.05785$ no ground screen present

$Wprime0 := (1 + Rv0) \cdot \frac{G0h}{2}$ $|Wprime0| = 0.03874$ with perfect ground screen

$G := 20 \cdot \log\left(\left|\frac{Wprime}{Wprime0}\right|\right)$ $G = 3.4822$ dB field strength improvement in dB with perfect ground screen and antenna at its minimum height

---

For ground screen with dielectric layer

Properties of the dielectric layer

$EPSd := 2.6$ $SIGMAd := 0.0$ $nnd := EPSd - i \cdot 1.7975510^{10} \cdot \frac{SIGMAd}{f}$

$ZNORM_n := i \cdot \tan\left(k \cdot t_n \cdot \sqrt{nnd - \cos(\Psi)^2}\right) \cdot \frac{\sqrt{nnd - \cos(\Psi)^2}}{nnd}$ modified normalized surface impedance

$Rv_n := \frac{\sin(\Psi) - ZNORM_n}{\sin(\Psi) + ZNORM_n}$ reflection coefficient

$Zaprime_n := ZNORM_n - ZNORM0$

$\Omega aa_n := Zaprime_n \cdot \Omega n$

$Wpp_n := (1 + Rv0) \cdot \frac{G0h + \Omega aa_n}{2}$

$Gp_n := 20 \cdot \log\left(\left|\frac{Wpp_n}{Wprime}\right|\right)$ field strength with dielectric covered ground screen relative to perfectly conducting ground screen

Plot of field strength enhancement as a function of dielectric layer thickness

$s = 0.0508$ $EPS = 4$ $SIGMA = 0$ $EPSd = 2.6$ $SIGMAd = 0$

$h = 2.54 \cdot 10^{-4}$ height of dipole above surface

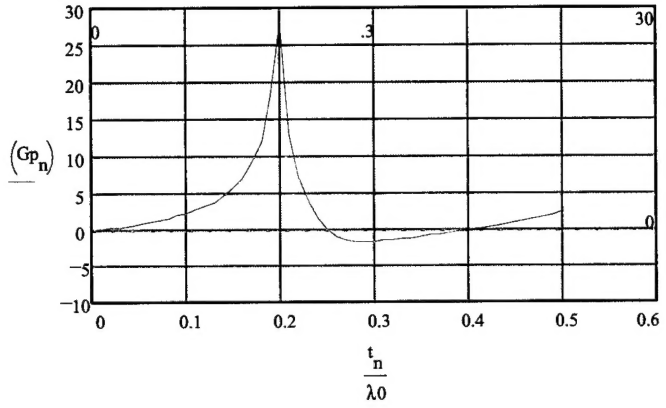

Plot of ZNORM as a function of dielectric layer thickness

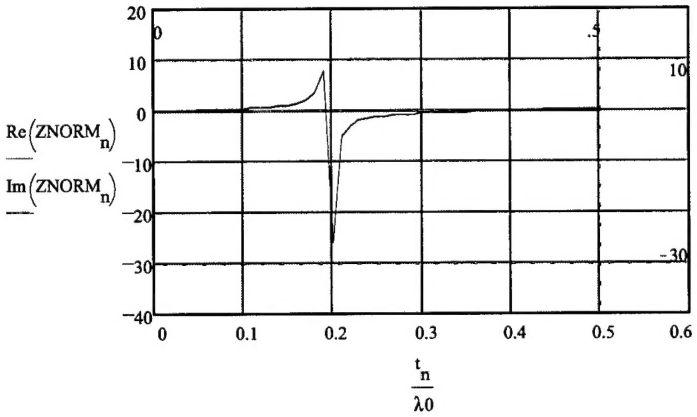

Plot of sigma as a function of dielectric layer thickness

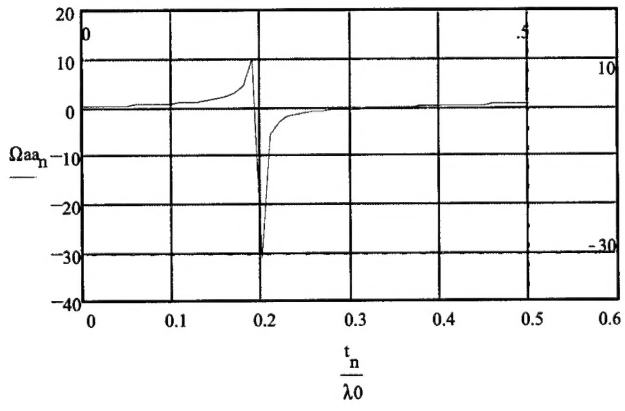

APPENDIX C:

This MathCAD document row_diel_layer_pattern.mcd allows the computation of the elevation patterns for a dielectric covered ground screen. The top of the layer is level with the bare earth. Wait's theory is used.

The integrals defined by Wait are evaluated with the angle of the observer incremented for a circular ground screen of a given surface impedance. The antenna height h cannot be equal to zero.

$f := 3.0 \cdot 10^9$ frequency in Hz $\lambda 0 := \frac{2.9979610^8}{f}$ $\lambda 0 = 0.099932$ wavelength

$s := 0.0508$ radius of ground screen in meters (set to 2")

$k := 2 \cdot \frac{\pi}{\lambda 0}$ $k = 62.87461$ propagation constant in free space

$ks := \frac{2 \cdot \pi}{\lambda 0} \cdot s$ $ks = 3.19403$

$n := 1, 2 .. 89$ increment number of elevation angles

$\Psi\Psi_n := n$ elevation angle of observer in degrees

$\Psi_n := \Psi\Psi_n \cdot \frac{\pi}{180}$ elevation angle in radians

$v_n := \cos(\Psi_n)$

$h := 0.000254$ height of antenna above perfectly conducting scree and dielectric surface

$w := h \cdot k$

$t := 0.016$ thickness of the layer over the perfect ground screen $\frac{t}{\lambda 0} = 0.16011$

Note: w cannot be set to zero in the integral I2 below

$F(u,n) := e^{\left(-i \cdot \sqrt{u^2+w^2}\right)} \cdot J1\left(u \cdot v_n\right) \cdot \left(\frac{u^2}{u^2+w^2}\right)$ Evaluate Wait's integral by parts

$I1_n := \int_0^{ks} F(u,n)\, du$

$I2_n := \left(\frac{1}{i}\right) \cdot \int_0^{ks} \left(\frac{1}{u}\right) \cdot F(u,n)\, du$

$I_n := I1_n + I2_n$

$\Omega_n := \left(\frac{1}{v_n}\right) \cdot I_n$

Bare earth properties: $EPS := 4$ dielectric constant $SIGMA := 0$ conductivity

$$nn := EPS - i \cdot 1.7975510^{10} \cdot \frac{SIGMA}{f} \qquad nn = 4$$ refractive index of earth squared

$$ZNORM0_n := \frac{\sqrt{\left(nn - \cos\left(\Psi_n\right)^2\right)}}{nn}$$ normalized surface impedance of the bare earth

$$Rv0_n := \frac{\sin\left(\Psi_n\right) - ZNORM0_n}{\sin\left(\Psi_n\right) + ZNORM0_n}$$ reflection coefficient from bare earth at antenna height h

$$G0h_n := \frac{e^{i \cdot k \cdot h \cdot \sin\left(\Psi_n\right)} + Rv0_n \cdot e^{-i \cdot k \cdot h \cdot \sin\left(\Psi_n\right)}}{1 + Rv0_n}$$

$$\Omega a_n := \Omega_n \cdot \left(-ZNORM0_n\right) \qquad \Omega a_1 = 0.39354 + 0.52948i$$

is the gain factor for a perfectly conducting circular ground screen with the antenna at its given height. If it is << Goh then the screen has a small effect on the field strength. If it is >> Goh then the screen has a significant effect.

$$Wprime_n := \left(1 + Rv0_n\right) \cdot \frac{G0h_n + \Omega a_n}{2} \qquad \left|Wprime_1\right| = 0.05785$$ no ground screen present

$$Wprime0_n := \left(1 + Rv0_n\right) \cdot \frac{G0h_n}{2} \qquad \left|Wprime0_1\right| = 0.03874$$ with perfect ground screen

$$G_n := 20 \cdot \log\left(\left|\frac{Wprime_n}{Wprime0_n}\right|\right) \qquad G_1 = 3.4822 \text{ dB}$$ field strength improvement in dB with perfect ground screen and antenna at its minimum height

---

For ground screen with dielectric layer

Properties of the dielectric layer

$EPSd := 2.5$ $SIGMAd := 0.0$ $$nnd := EPSd - i \cdot 1.7975510^{10} \cdot \frac{SIGMAd}{f}$$

$$ZNORM_n := i \cdot \tan\left(k \cdot t \cdot \sqrt{nnd - \cos\left(\Psi_n\right)^2}\right) \cdot \frac{\sqrt{nnd - \cos\left(\Psi_n\right)^2}}{nnd}$$ modified normalized surface impedance

$$Rv_n := \frac{\sin\left(\Psi_n\right) - ZNORM_n}{\sin\left(\Psi_n\right) + ZNORM_n}$$ reflection coefficient

$$Zaprime_n := ZNORM_n - ZNORM0_n \qquad \Omega aa_n := Zaprime_n \cdot \Omega_n$$

$$Wpp_n := \left(1 + Rv0_n\right) \cdot \frac{G0h_n + \Omega aa_n}{2} \cdot \cos\left(\Psi_n\right)^2$$

$$Gp_n := 20 \cdot \log\left(\left|\frac{Wpp_n}{Wprime_n}\right|\right)$$ field strength with dielectric covered ground screen relative to perfectly conducting ground screen

Plot of field strength enhancement as a function of elevation angle

$s = 0.0508$ $EPS = 4$ $SIGMA = 0$ $EPSd = 2.5$ $SIGMAd = 0$

$h = 2.54 \cdot 10^{-4}$ height of dipole above surface $t = 0.016$ wavelengths

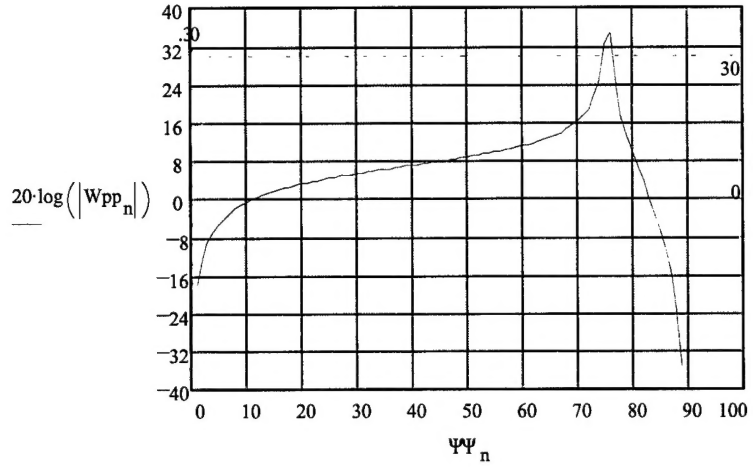

Write data to file:

WRITEPRN(patt1) := $20 \cdot \log(|Wprime0_n|)$

WRITEPRN(angle) := $\Psi\Psi_n$

WRITEPRN(gain1) := Gp_n